ELSEVIER

Contents lists available at ScienceDirect

# **Automation in Construction**

journal homepage: www.elsevier.com/locate/autcon



# Rebar detection and localization for bridge deck inspection and evaluation using deep residual networks



Habib Ahmeda,\*, Hung Manh Laa, Khiem Tranb

- <sup>a</sup> Advanced Robotics and Automation (ARA) Lab, Department of Computer Science and Engineering, University of Nevada, Reno, United States
- <sup>b</sup> Department of Civil and Coastal Engineering, University of Florida, Gainesville, United States

#### ARTICLE INFO

# Keywords: Non-destructive evaluation (NDE) Structural health monitoring (SHM) Ground penetrating radar (GPR) Rebar detection and localization Convolutional neural network (CNN) Residual networks (ResNets)

#### ABSTRACT

Structural Health Monitoring (SHM) and Nondestructive Evaluation (NDE) of civil infrastructure has been an active area of research for the past few decades. Due to rising costs, safety issues and error of human inspection methods, automated methods for bridge inspection and maintenance are being proposed. The purpose of this research is to develop an automated rebar detection and localization system utilizing supervised (Deep Residual Networks) and unsupervised (K- means clustering) techniques. Data has been collected from nine bridges using Ground Penetrating Radar (GPR) sensors. The performance of the proposed rebar detection and localization system has been evaluated on a wide-range of performance metrics, which emphasize the superior performance of the proposed technique over existing methods. The results reveal positive correlation between number of layers of networks, training time and other performance metrics. The overall performance of the proposed system is also dataset-dependent with factors such as noise artefacts, reflections and visual quality of rebar profiles.

#### 1. Introduction

The monitoring, maintenance and rehabilitation of civil infrastructure is of paramount importance at the national and international level. Of the different types of civil infrastructure, the need for maintenance and evaluation of bridges has been stressed by studies in the recent past [1–4]. According to the National Bridge Inventory (NBI) statistics, there are more than 307,000 bridges in the entirety of the United States [5]. Although, the overall ratio of marginally or seriously damaged bridges has been declining over the past few decades, the recent statistics outlined by the US Department of Transportation have classified around 67,000 bridges as structurally deficient and 85.000 as functionally obsolete in nature [5]. Out of the \$14.3 billion expenditure sanctioned for maintenance of existing bridges and construction of new bridges in 2010, \$12.8 billion was dedicated towards the maintenance of existing bridges [6], which shows that a considerable portion of annually allocated funds are being diverted for the maintenance of bridges. The primary motivations for conducting this research can be broken down into two parts, namely: (i) the need for robotic automation to improve the cost-effectiveness and efficiency of the different processes underlying non-destructive evaluation of bridges, and (ii) the importance of including GPR data from different bridges to develop a robust rebar detection and localization system.

The first motivation is to ensure that novel automation solutions can be proposed, which can replace the existing methods that are errorprone and financially inefficient in nature. Lack of adequate attention towards maintenance and monitoring of bridges can lead to disastrous incidents. A number of different factors contribute towards the partial or total destruction of bridges, ranging from design errors and construction defects to environmental degradation, scour, flood, collision and overloading [7,8]. The impact of bridge destruction and collapse far exceeds the overall material and financial costs associated with the bridge construction, as it also includes the various direct and indirect costs, which include, but are not limited to loss of lives, user delays, planning for alternate routes, along with the greenhouse gas emissions linked to detours and delays in traffic [7,9.10,11]. Fig. 1 highlights some of the multitude of prior tragedies in the wake of bridge destruction incidents in the US. It is being predicted that with the increase in climate change and frequency of adverse climate incidents (e.g. hurricane, floods, tsunamis) on a global scale, the overall costs related to repairing is also expected to accelerate from \$140 billion to \$250 billion annually [10] with direct and indirect losses amounting to more than 17% of the total costs [11]. Therefore, the timely evaluation, monitoring and rehabilitation of bridges can result in reduced overall direct costs as well as the indirect costs in terms of potential destruction of property and lives in the wake of bridge destruction. For the purpose

E-mail address: hahmed@nevada.unr.edu (H. Ahmed).

<sup>\*</sup> Corresponding author.



Fig. 1. Some of the serious recent bridge accidents in the US: (a) A collapsed railroad bridge in Alabama that resulted in around 47 deaths. (b) Collapsed bridge that connected Point Pleasant, West Virginia with Gallipolis, Ohio [1].

of bridge monitoring and evaluation, the different techniques for NDE have the potential towards minimizing the overall direct and indirect costs associated with destruction of bridges caused by internal deficiencies, construction deficits and maintenance-related issues. In the light of this realization, a number of national-level initiatives have been developed in the United States. One such example is the Long-Term Bridge Performance Program (LTBP) initiated by the Federal Highway Administration (FHWA) with the primary aim towards promoting the utilization of non-destructive evaluation technologies and techniques for regular bridge inspection and maintenance [12].

Another important motivation for this research is related to the incorporation of data from multiple bridges. Many of the relevant studies do not effectively highlight the various properties of the GPR data from the different bridges that has been collected. It can be seen from some of the dataset examples given in Fig. 2 that the different physical properties (e.g. physical dimensions, use of construction materials, depth of steel rebars and spacing between individual rebars) within the different bridges can lead to varying results obtained using GPR radargram. The usage of data from diverse bridges is particularly important for rebar detection and localization systems that employ deep neural networks, as in the case of this research. According to this rationale, this research has utilized data from different bridges, which provide a diverse set of data with varying physical properties that allow the development of a robust rebar detection and localization system.

There are a number of ways in which this study improves on the state-of-the-art, which include the following:

- A novel method for rebar detection and localization, which leverages supervised (i.e. Deep Residual Networks) and unsupervised (i.e. K-means clustering) learning-based techniques.
- The incorporation of challenging dataset from nine real bridges with varying data properties; the data from many of the bridges have not been used in any prior studies.
- Majority of relevant studies provide examination of a single Deep learning framework. In this research, the effect of different network parameters (e.g. number of layers, batch size and epochs for system training) of the different Deep Residual Networks (ResNet-18, ResNet-34, ResNet-50, ResNet-101, ResNet-152, DenseNet-121, DenseNet-161) has been examined on the overall performance of the rebar detection and localization system.
- A comprehensive discussion on performance evaluation has been provided, which shows that the performance of proposed method is superior or at par with recently developed techniques. A comparison with existing studies has revealed that this study employs a widerange of performance metrics that have not been used in the relevant researches in the past.
- Unlike earlier studies, this study also provides a detailed examination of different challenges and the manner in which it affects the overall performance of the rebar detection and localization systems.

#### 2. Related works

The non-destructive evaluation (NDE) of civil infrastructure has been a widely-discussed research area in the past. In order to do adequate justice to the different tools, techniques, methodologies and technologies used by the prior studies related to NDE of bridges, the proceeding discussion will be divided in terms of variations in existing studies related to: (i) a general overview of literature on different tools and techniques for NDE of infrastructures, (ii) literature particularly emphasizing towards developing methods for rebar detection and localization for bridges. A comprehensive overview of the recent and relevant literature has been also provided in [13]. Fig. 3 effectively outlines the different ways in which the prior studies have been extending the state-of-the-art in the literature pertaining to bridge inspection in particular and civil infrastructure in general.

# 2.1. General overview of techniques for NDE of infrastructures

Traditionally, infrastructure evaluation has been considered a manual task, which has been carried out by civil personnel using primitive sensors for data collection [8]. In the recent past, a number of different robotic platforms have also been introduced for the purpose of infrastructure evaluation to enhance the overall efficiency and reduce the time-consumption and error in data collection. A wide array of diverse robots have been developed ranging from climbing robots (e.g. legged-robots, wheel-based sliding robots and crawler robots) [14–29], and multi-rotor unmanned aerial vehicles (e.g. quad-rotors and octorotors) [30-37] to unmanned ground vehicles (UGVs) (e.g. ARA Lab Robot., ROCIM, RABIT) [38-49] and water-based robotic crafts (e.g. unmanned submersible vehicles (USVs), underwater marine vehicles (UMVs), underwater vehicles (UUVs)) [50-53]. Robotics Assisted Bridge Inspection Tool (RABIT) is designed for an efficient automated defect detection of bridge decks [12,48,53,54] with state-of-the-art sensor technologies (e.g. impact echo, ultrasonic surface waves, electrical resistivity and GPR). A multi-functional, multi-sensor-based mobile platform (i.e. ARA Lab platform) for the evaluation and inspection of civil infrastructure [8,55] has been developed recently. Due to the inherent flexibility of most robotic platforms, majority of these platforms can be utilized for SHM of wide-range of different civil infrastructures.

Apart from development of novel robotic platforms for SHM, considerable research focus towards concrete crack detection [14,20,53,55,56–59]. Some of the earlier works focused on the utilization of basic-level image processing techniques for crack detection in concrete structures [14] [20] [53]. A block-based crack detection approach was developed for bridge decks in another study [55]. A genetic learning-based network optimization algorithm was also proposed with application for concrete crack detection [58]. In order to overcome some of the limitations of basic-level image processing techniques, the use of different Deep Learning frameworks has also been proposed for crack detection [57] [59] [60] [61] [62]. The use of encoder-decoder-

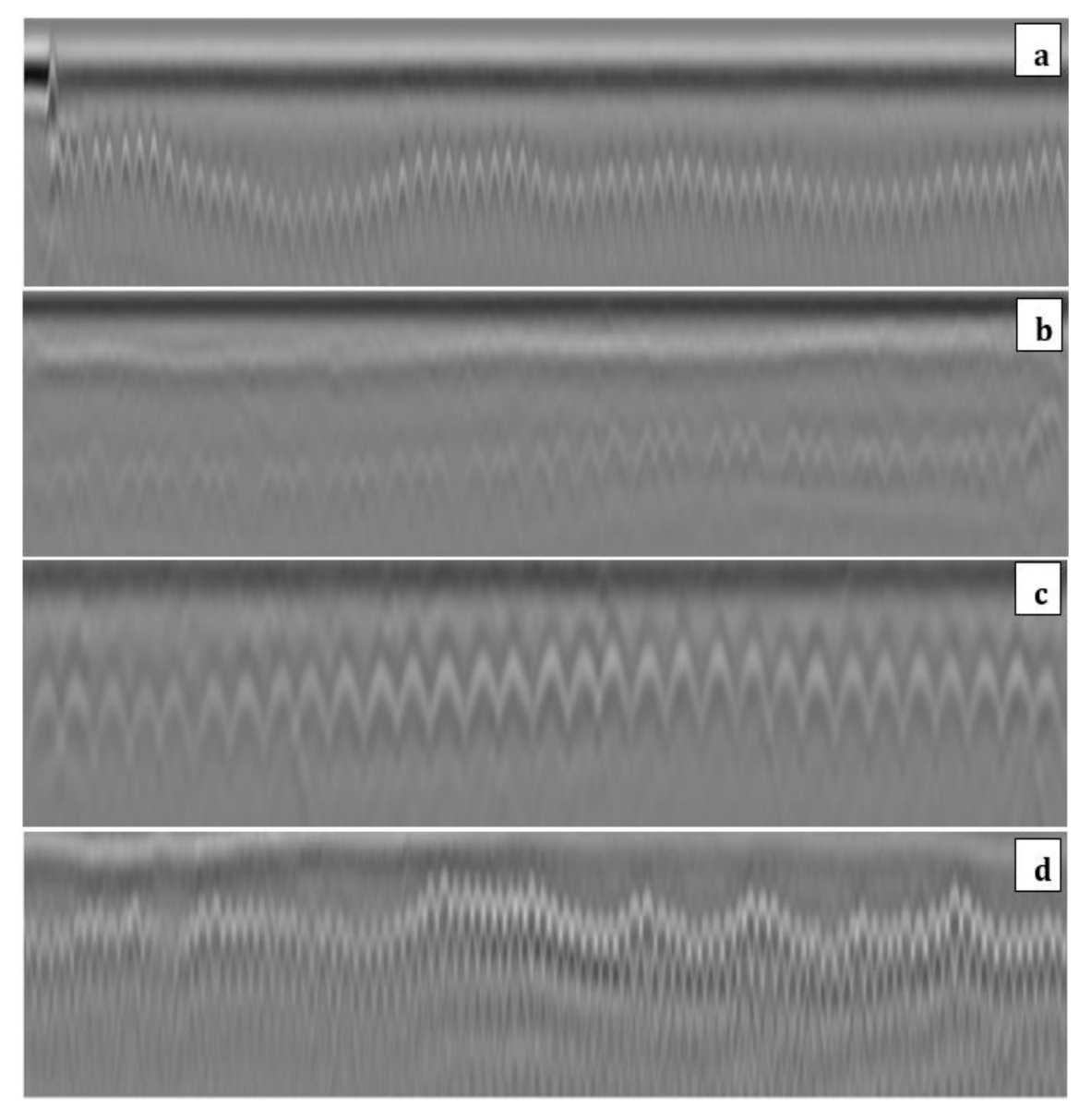


Fig. 2. Diversity of data obtained from the different bridges used in this research from the following bridges: (a) East Helena Bridge, (b) Dove Creek Bridge, (c) Warren County bridge and (d) Fordway Bridge.

based Deep learning architecture was able to improve the existing limitations using a pixel-wise classification of images [59]. Using data from various concrete structures captured in different lighting conditions, Cha [60] leveraged Deep learning-based model for concrete crack detection. Another study made use of damage quantification using depth-based camera and Faster R-CNN model for SHM of concrete structures [61]. The use of Deep-learning-based techniques was also used for developing image transformation method for sewer inspection to transform GPR scans into sub-surface permittivity maps [63]. For the classification of underground objects using GPR data, a 3D CNN model was proposed in another recent study [64].

### 2.2. Methods for rebar detection and localization

The usage of GPR data for infrastructure evaluation has been in practice for as far back as the 1970s with applications that include void space detection, depth of concrete cover on bridges, locating metallic objects in concrete spaces, and general inspection and maintenance of reinforced concrete structures [65]. Some of the earlier studies have used GPR data for underground pipe detection [66], as well as detection

of various buried objects, e.g. landmines and pipes [67]. It is only recently that the shift has focused towards using GPR for bridge evaluation with particular emphasis on rebar detection and localization [48] [65] [68] [69] [70]. For the case of bridge monitoring, one of the earlier studies utilized GPR data for rebar detection in bridge decks [65]. This particular study made use of partial differential equations and template matching technique with sum of square similarity index for hyperbola localization [65]. The different existing techniques for rebar localization can be broadly classified into bounding-box and hyperbola interpolation-based approaches. For hyperbola interpolation in the context of rebar localization, RANSAC and Hough transforms are frequently employed [48] [67].

Another research by Gibb and La [68] proposed a method for rebar detection using Naïve Bayesian classifier trained on HOG features for rebar detection, along with the precise hyperbola localization algorithm for rebar localization. Kaur et al. [48] developed an automated system for rebar analysis using Histogram of Oriented Gradients (HOG)-based features and Support Vector Machines (SVM) for recognition and classification of rebar and non-rebar images. Another recent study by Dinh et al. [71] proposed a novel method for rebar detection, which involved

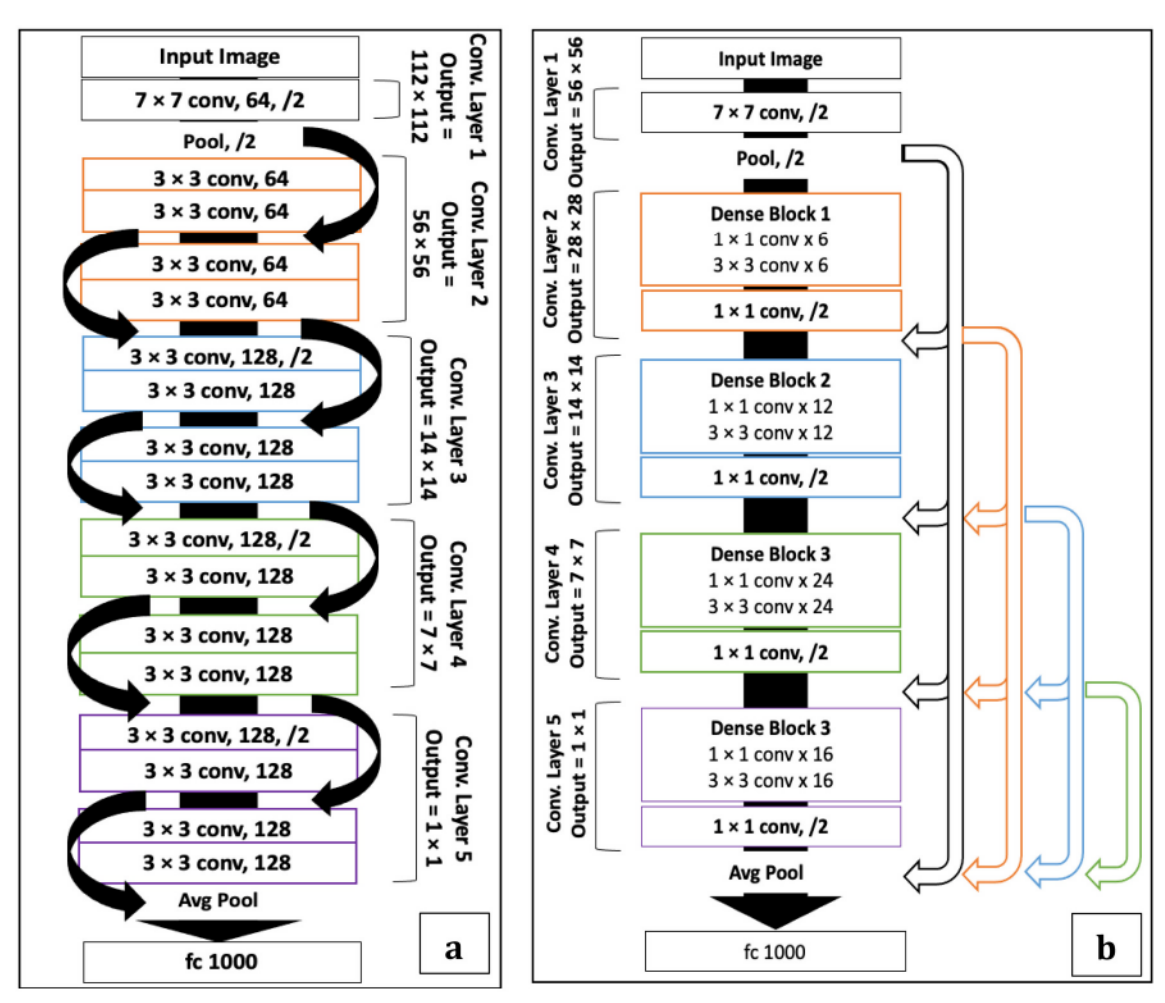


Fig. 3. Some of the Deep Architectural frameworks used in this study: (a) ResNet-18 [75], and (b). Densenet-121 [76].

the usage of Convolutional Neural Networks (CNNs). A number of different methods have been deployed for the case of rebar detection, but most of the earlier studies on rebar localization attempt to leverage the hyperbolic signatures [65] [68]. In the following section of the discussion, some of the salient features of the proposed rebar detection and localization method will be discussed.

#### 3. System methodology

In this section, a comprehensive evaluation of the different processes within the proposed method for rebar detection and localization will be performed. Earlier studies focusing on rebar detection and classification have used a number of different methods, ranging from Support Vector Machines [48] and Naïve Bayesian classifier [68] to primitive Neural networks in some of the early studies using GPR [66] [67]. One of the recent studies by [71] has utilized a convolutional neural network for rebar detection. From a machine learning perspective, the detection and recognition of rebar from other non-rebar anomalies and artefacts detected in B-scans can be considered as a twoclass classification problem. Earlier studies employing Residual Networks and their variants have attested to their superior performance towards tackling a vast range of research problems [72] [73] [74]. To the knowledge of the authors, there is no single work in the past, which has provided a comprehensive and detailed evaluation and analysis of Deep Residual Networks (ResNet) towards rebar detection and localization. It is for this reason this study has leveraged different pre-existing ResNet frameworks (e.g. ResNet-18, ResNet-34, ResNet-50, ResNet-101, ResNet-152). Residual Networks have shown high performance on diverse applications, which will be highlighted in the next sub-section. Although, a preliminary analysis has been introduced in recent works by the authors [69] [70]. However, it lacks the depth and clarity warranted towards investigating Deep Learning models developed in the recent years. In contrast to these earlier works, this research will essentially be a continuation and in-depth evaluation of the performance of Deep Residual Networks, along with its various pros and cons for the application of rebar detection in bridges. Fig. 3 highlights the two Deep Learning architectures, which have been used in this study. namely ResNet-18 and DenseNet-121. A number of different ResNet architectures (e.g. ResNet-18, ResNet-34, ResNet-50, ResNet-101, ResNet-152) are used to assess the effect of different network parameters (e.g. number of epochs, batch size, and number of layers) on the performance of proposed rebar detection and localization system. The performance of the high performing ResNet (e.g. ResNet-101, ResNet-152) is compared with DenseNet architectures (e.g. DenseNet-121, DenseNet-161).

#### 3.1. Background on deep residual networks

Ever since its inception in the recent past, the Deep Residual Networks [75] [77] have gained a considerable amount of attention, as a state-of-the-art Deep Convolutional Networks framework, which provides reliable performance and robustness in diverse applications. The seminal research outlining the efficacy of this particular Deep Learning model on various image recognition competitions highlighted the rectification of various limitations (e.g. vanishing/exploding gradients, degradation) pertaining to performance of traditional Deep

Convolution Neural Network (CNN) models, especially with increase in the depth or number of layers [75]. It is for this reason that a wide range of different applications have been successfully developed in a diverse field of research, ranging from medical imaging and diagnostics [72], remote sensing applications [73], steganography [78], image super-resolution [74], video-based human action recognition [79] to optical flow estimation [80], image de-blurring [81], hyperspectral imaging [82] as well as fault analysis and diagnostics [83].

Another area of emphasis of recent studies is towards proposing modifications of the original Residual Network architecture (i.e. ResNet-50) in order to leverage its benefits in terms of performance and efficiency as well as cater to other application-specific challenges. For example, a two-stage framework for melanoma was proposed in one of the recent study, which included fully-connected Residual Network with multi-scale contextual information [72]. For the case of image super-resolution, the original Residual block was modified in order to provide a multi-scale residual block, which was able to enhance the performance of the developed system [84]. A two-stream motion and appearance information processing Residual network was also proposed for video-based human action recognition [79]. For image classification tasks, it was demonstrated that by using dilation layers in the overall ResNet architecture, the overall output resolution and classification performance was improved considerably [72]. Similarly, the use of single-image-based super-resolution method was improved by merging the upscaling module within the residual framework to propose a Deep upscaling framework with improved performance over state-of-the-art [74]. A multiple layer of residual networks, namely the Residual of Residual (RoR) network was proposed in another recent study with multiple layers of shortcut connections that resulted in improved performance on benchmark dataset (e.g. CIFAR-10, CIFAR-100, SVHN) [85]. By combining the positive elements of the two different networks, namely the ResNet [75] and U- Net [58], a deep ResUnet framework was developed in another recent study, which was successfully tested towards the detection and extraction of roads in remote sensing images [48]. Table 1 outlines the different Deep Learning architecture employed in the relevant research area with their different model properties. It can be seen that unlike other studies, this research employs a wide-range of different ResNet and DenseNet models.

#### 3.2. GPR data collection

In this study, data collected using GPR sensor has been used as input for the rebar detection and localization systems. The purpose of this sub-section is to provide a brief overview of the salient features of the GPR data collection processes. GPR and the associated data has been widely used for conducting geological surveys on a number of different

Table 1
Comparison of the different Deep Learning architectures used in relevant studies

Study	Applications	Network Architecture	Network	Network Characteristics		
		Architecture	Depth	Parameter		
[64]	Underground object classification	3D-CNN	3	N/A		
[86]	Bridge damage detection	DINN	20	24.8 million		
[60]	Concrete crack	CNN	8	N/A		
[61]	detection	Faster-R-CNN	16	N/A		
This study	Rebar detection and	ResNet-18	18	11.2 million		
	localization	ResNet-34	34	21.3 million		
		ResNet-50	50	23.5 million		
		ResNet-101	101	42.5 million		
		ResNet-152	152	58.2 million		
		DenseNet-121	121	~4 million		
		DenseNet-161	161	~18 million		

terrains, ranging from analysis of glacial deposits [87] [88], faults [89] [90], and peatland [91] [92], to coastal regions [93] [94], delta [95] and lunar explorations [96] [97]. At the same time, data collected from GPR sensors have also been extensively employed for NDE of different civil infrastructures [8] [12] [55] [54] [69] [70] and detection of various terrain-level and underground features (e.g. underground pipes, cables, landmines, tunnel defects, buried objects) [65] [68] [66] [67] within civil engineering and civil surveying tasks. The principles underlying the data collection using GPR sensors have been given in Fig. 4. In typical inspection operations, the electromagnetic (EM) waves with a frequency between 10 MHz and 5 GHz is transmitted into the sub-surface using mono-static GPR antennas as the primary transmission device [98]. As, the EM waves progress through the different layers of the underground sub-surfaces with varying dielectric properties, these waves undergo changes in velocity, which are dependent on the dielectric constant and electrical conductivity of the different sub-surface layers [98]. This phenomenon has been highlighted in Fig. 4(a). Slight variations in the dielectric properties of the sub-surface layers can lead to partial reflection of the originally transmitted EM waves, which are amplified and recorded by the receiving antennas. The different factors that affect the dielectric constant for any specific material is dependent on moisture content, porosity, texture, chemical composition and density [98] [99]. For the detection of different underground objects (e.g. buried objects, landmines, steel pipes, cables, metal objects, archaeological sites) within different types of subsurface media (e.g. sand, clay, wood, concrete, body of water, oil, ice), there are a number of different variables that need to be taken into consideration.

The value for dielectric permittivity  $k_m$  is selected based on the composition of the underground material m [100]. Typically, the value for  $\nu$  which is given in eq. (1) is specified as 0.2998 m/ns [100]. The eqs. (1)–(3) have been given along with supporting mathematical evidences and technical details in [100]. Following are some of the mathematical equations governing the calculation of these variables, which include wavelength in air  $\lambda_a$ , wavelength in specific material  $\lambda_m$ , central frequency  $f_c$  and maximum sampling interval t for the different antennas being used:

$$\lambda_a = \frac{v}{f_c} \tag{1}$$

$$\lambda_m = \frac{\lambda_a}{\sqrt{k_m}} \tag{2}$$

$$t = \frac{1000}{6f_c} \tag{3}$$

Depending on the type of application for which the GPR data is being collected, a number of different approaches for data collection have been employed in the past, which include common mid-point, fixed off-set profiling and reflection profiling-based approaches [101] [102] [103] [104]. Fig. 4 highlights the different approaches and the ways in which the transmitter and receiver positions change over time. Fig. 4(a) provides a visualized effect of different sub-surface layers on the velocity of the transmitted and received EM waves. Fig. 4(b) highlights the fixed offset profiling method for GPR data collection with the GPR transmitter and receiver collectively moving in a linear fashion to cover the underground mapping of the desired region. It can be seen from Fig. 4(b) that presence of anomalous underground object can lead to variations in the reading by the receiver over time. In Fig. 4(c), the common midpoint position method has been highlighted, which shows that the transmitter and receiver move further apart as the data collection progresses from the initial points  $T_1$  and  $R_1$  to the final points  $T_n$ and  $R_n$  (details regarding the system parameter adjustment and best practices for GPR using fixed offset-based profiling method, see [101] [103] [105]). In the following sub-section, the salient features of the proposed method for rebar detection and localization will be outlined.

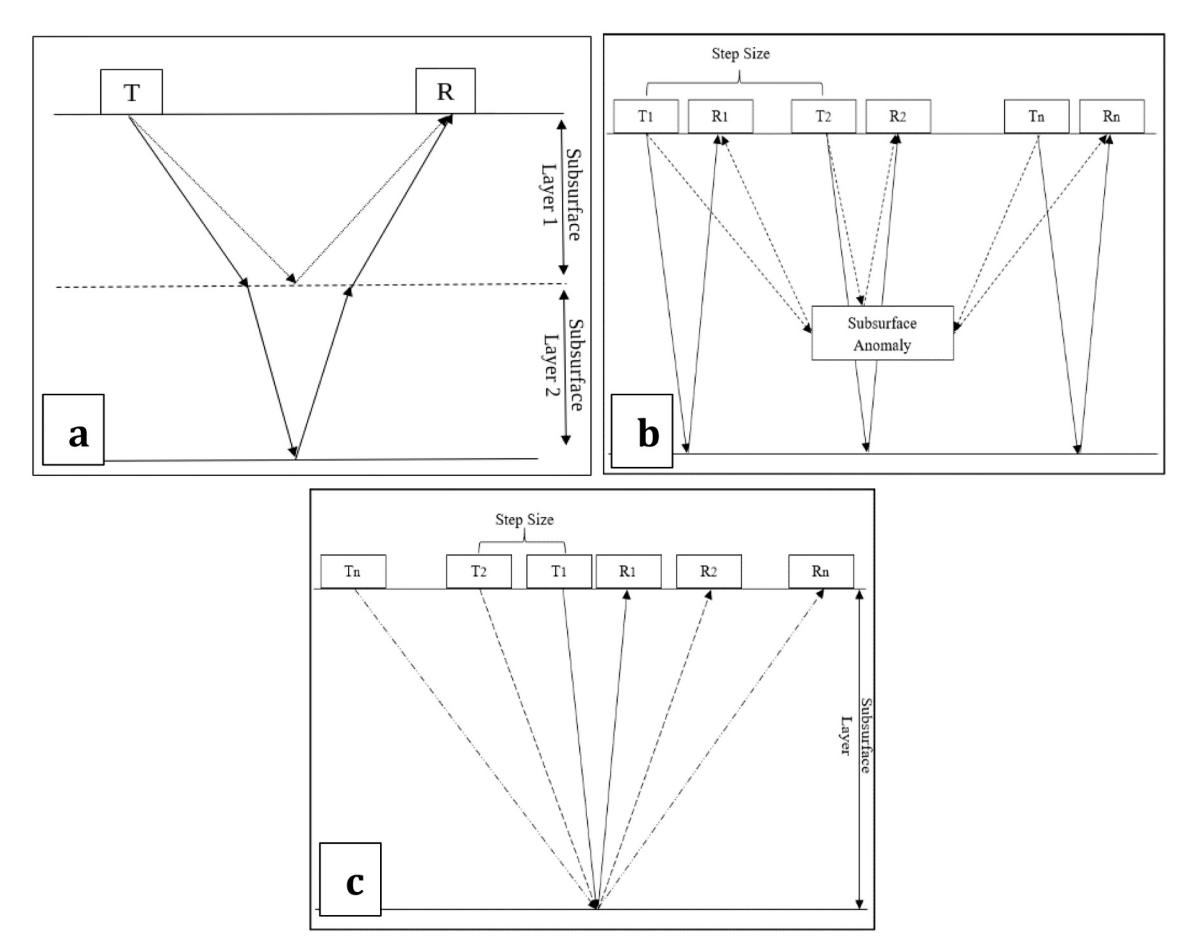


Fig. 4. Principles of GPR data collection using different methods: (a) the transmission and reception of radar waves from different sub-surface layers, (b) fixed-offset reflection profiling method, (c) midpoint position method starting from transmitters and receivers at T<sub>1</sub> and R<sub>1</sub> to T<sub>n</sub> and R<sub>n</sub> [98].

# 3.3. Proposed method for rebar detection and localization

In this section, a detailed examination of the proposed rebar detection and localization system will be provided. Earlier discussion has shed light on some of the most important recent works towards rebar detection and localization. A number of different techniques have been proposed for the development of rebar detection system in the past, ranging from simple Neural Network implementations [66] [67] and 24-layer Convolutional Neural Network [71] to Support Vector Machine [48] and Naive Bayesian-based approaches [68]. In the proposed study for rebar detection, the use of Deep Residual Neural Network has been proposed [75]. Some of the preliminary works in this respect have been proposed in recent studies by the authors [69] [70]. This study will provide a comprehensive, in-depth analysis of different Deep Residual Network-based architectures (namely ResNet-34, ResNet-50, ResNet-101 and ResNet-152) for the development of rebar detection and localization system. There are a number of key objectives, which will be evaluated in this research. Despite the widespread use of Deep Learning architectures, there is a need for assessing their feasibility towards practical development and implementation on practical robotic systems for real-time bridge infrastructure evaluation [8] [12] [55] [54] [69] [70]. In this regard, there is a need to assess the ideal balance between network complexity (the complexity and computational requirements increase exponentially with increase in depth or number of layers of Deep layered architectures) and performance (measured in terms of accuracy, loss, time and computational requirements). This particular aspect will involve the use of Residual Networks for rebar detection system with the ultimate aim of developing practical infrastructure evaluation of bridges, which is currently lacking in the existing literature.

The findings in this study will provide valuable insights that can aid in the development of state-of-the-art Deep Learning-based systems with potential for practical implementation on real-time systems. The practical implementation will be carried out in the future after the successful validation and evaluation of the various performance-level trade-offs in this study. At the same time, a novel rebar localization system has also been proposed that will visually detect and highlight the location of rebar signatures within GPR radargram, which contains vital underground information regarding the presence of different buried objects (e.g. underground pipes, underground transmission cables, steel rebars and other construction material).

The localization of rebar signatures from GPR radargram is a crucial component of the overall accurate SHM for bridges using NDE-based methods that ensure the integrity of the bridge infrastructure. Instead of directly relying on raw GPR data, the proposed rebar localization system will allow the civil inspectors to focus their attention on rebar signatures in GPR radargrams, which can allow them to assess the overall level of deterioration of the individual steel rebars within the overall bridge infrastructure. Fig. 5 highlights the main components of the proposed rebar detection and localization system. Starting from the data collection process to discussion regarding rebar detection and localization system, which will conclude with the evaluation of performance of both systems using credible performance evaluation metrics. Based on Fig. 5, the proposed model for rebar detection and localization can be divided into three main sections, namely:

(i) GPR data collection: In the previous sub-section, a considerable level of theoretical detail has been outlined for data collection using GPR sensors. In this section, some additional details regarding the

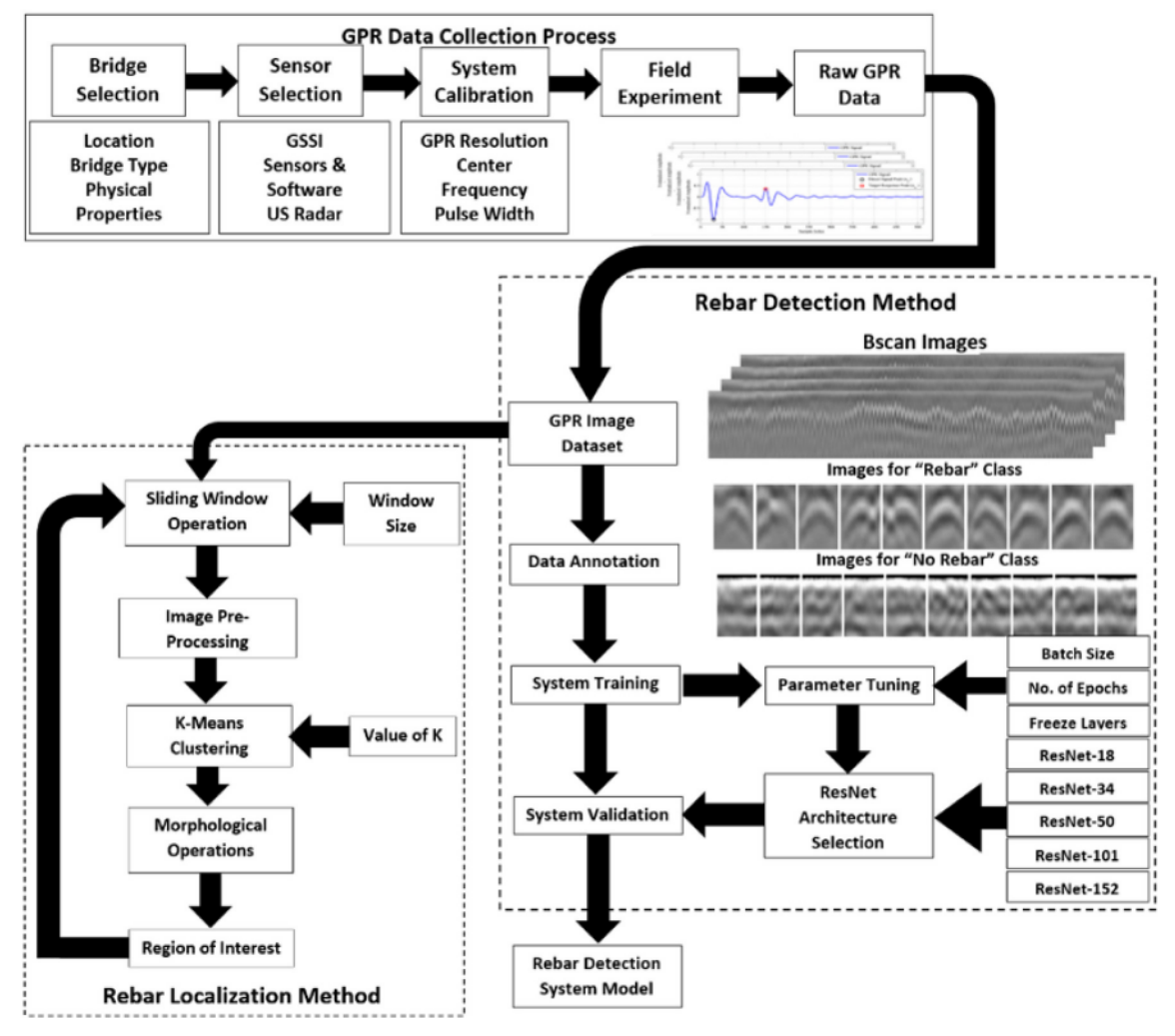


Fig. 5. Model for the proposed rebar detection and localization method.

practical implementations for data collection in this research will be discussed.

(ii). Rebar detection system: Some of the salient features of rebar detection method will be highlighted in the following sub-section, and.

(iii). Rebar localization system: The discussion in one of the subsection will also outlined the proposed method for rebar localization.

For the case of GPR data collection, the fundamental details are given in the previous section. Fig. 5 outlines some of the different steps undertaken from data collection using GPR sensor. The GPR data collection starts with bridge selection, which should take into account type of material, physical and geometric properties of bridge (i.e. length, width, height of bridge), bridge type (e.g. arch, beam, truss, girder bridges), and sensor used for data collection. The frequency at which GPR data is collected is dependent on the type and location of sub-surface reinforcements in bridges. Based on the type of application, there is a need for selection of appropriate GPR sensor for the relevant application. A number of different firms (e.g. GSSI [106], Sensors & Software Inc [107], US Radar Inc [108]) provide a wide- range of reliable GPR equipment for data collection. The GPR data collected in this study utilized the IDS Georadar® sensor equipment system [109]. Based on the physical and geometric properties (e.g. length, width and height) of the bridge being investigated, there is a need to make appropriate adjustment within the system, such as center frequency, GPR resolution, sampling interval and pulse width [100]. The mathematical details of the different variables have been outlined in eqs. (1), (2) and (3), which are given in the previous section. There are a number of different methods that can be employed for data collection using GPR sensors, as discussed in the previous sub-section. In the current research, the single-fold, fixed-offset reflection profiling method has been used, as it is the most widely employed method for GPR application related to civil infrastructure evaluation, especially when there is a requirement of high spatial horizontal resolution [104].

The rebar detection system utilizes different Deep Residual Network architectures (e.g. ResNet-34, ResNet-50, ResNet-101, ResNet-152) with varying network parameters (e.g. systems trained with different batch size, number of epochs and number of layers). The performance of the Deep Residual Network with the most optimal network configuration is compared with relevant DenseNet architectures (DenseNet-121, DenseNet-161) [76], which is another Deep Convolutional Network that has gained considerable attention in the recent past. The rebar localization algorithm performs the different image pre-processing functions to ensure that the smaller regions of GPR images can be used to extract the relevant rebar signatures. K-means clustering has been employed as an unsupervised form of learning algorithm, which enables the effective separation between the foreground and background regions within the GPR images. Due to the level of noise and other artefacts present in the GPR data, a number of different visual artefacts are also included in the foreground. In order to decrease the interference of noise and other artefacts, a number of different morphological operations are used, which ensure that the original image is converted into binary image with foreground regions separated from the background regions. With the use of morphological features, many

of the noise and other reflective signals are separated and bounding box is used to highlighted the rebar signature within the GPR images.

The details of the proposed rebar localization system have been highlighted in Fig. 5. The different processes for rebar localization and rebar detection systems are separate in nature, which means that they can work simultaneously towards providing the desirable output within the larger framework of the overall.

system. Rebar localization system employs elements of the rebar detection system to ensure that it is able to perform different image processing functions on the parts of the larger GPR images that contain rebar signatures. Due to the large-scale size of the GPR images obtained from the raw GPR scan data, the rebar localization algorithm only works on portions of the GPR image using the sliding window-based approach. In the following section of the paper, the focus will be towards highlighting the effectiveness of the proposed rebar detection and localization method.

#### 4. Results

In this section, a comprehensive detail regarding relevant data and its subsequent analyses will be provided, along with visualization and supporting discussion to provide a detailed evaluation of the overall performance of the proposed system. At the same time, the various factors will also be highlighted that affect the overall performance of the proposed system for rebar detection and localization. Prior to the discussion related to performance of the rebar detection and localization system, there is a need to shed light on the data used for the training and validation of the proposed system, which will be discussed in the following sub-section.

#### 4.1. Dataset

For the development of the proposed system for rebar detection and localization, GPR data was acquired from a number of different bridges in the US. It can be seen from Table 2 that dataset 1 has been acquired from a bridge located in Warren County, NJ, which was included as part of the data within one of the earlier studies [48]. Since, the original source failed to mention the actual location of the bridge, it is for this reason that the dimensions and other physical properties of the bridge are not known. According to the knowledge of the authors, this dataset is the only publicly-available bridge dataset using GPR sensors. It can be seen from Table 2 that the bridge data has been taken from different type of bridges (e.g. suspension, beam, truss, girder). The physical dimensions vary considerably, ranging from the largest bridge in the dataset (i.e. Broadway Bridge, AR) spanning to a length of around 2786 ft. and the smallest in length being the Dove Creek Bridge, BC with a length of 50 ft. Table 2 outlines the important properties of the different bridges in terms of the bridge name, geographical location, and physical properties of the different bridges.

Table 3 highlights the quantity of images acquired from the different dataset. A major part of the GPR data (i.e. dataset 2 and 3) used

**Table 3**Data distribution of three datasets between training and validation sets.

Name	Class Rebar		Class No Re	Total	
	Training	Validation	Training	Validation	Total
Dataset 1 Dataset 2 Dataset 3 Total	1043 1200 7562 9805	228 300 1000 1528	7027 2400 8859 18,286	2040 600 1000 3640	10,338 4500 18,421 33,259

in this research is one segment of the overall GPR data collected from the inspection and evaluation performed on 40 different bridges in the United States between the time period of 2013 and 2014 [8] [12]. A portion of the collective GPR data (i.e. dataset 2) has also been used in previous studies [68] [69] [70]. Dataset 2 contains GPR data from four different bridges. It can be seen in Table 1 that the overall number of images in dataset 1 is considerably higher in comparison to dataset 2. Dataset 3 is a novel dataset that has not been used in any other studies in the past. It also contains data from four different bridges. All of the data was collected using RABIT platform in an automated fashion (for details regarding data collection, see [8] [12]). The additional data will ensure that the proposed rebar detection and localization is able to provide reliable performance for bridges with different physical properties. In terms of quantity, this dataset provides a reasonable amount of data, which can be used with Deep Learning-based algorithms to provide a foundation for development of reliable and robust rebar detection and localization system.

#### 4.2. Rebar detection method

In order to adequately assess the results that are presented in this sub-section, there is a need to understand the manner in which the testing and evaluation of the proposed model was performed. Firstly, the different dataset (i.e. dataset 1, 2 and 3) will be trained and tested individually on the designated Deep Learning model. The results will provide valuable insights in relation to optimizing the different learning parameters and their effect on the overall performance of the developed system for rebar detection. Secondly, the performance of the rebar detection system will be evaluated by separating the collective dataset into training and validation sets (i.e. six bridges for training and three bridges for validation), which will prompt further inquiry towards analyzing the robustness of the developed system towards unseen bridge data. Thirdly, in order to highlight the effects of computational resources on the proposed rebar detection system, two separate PC systems with different set of configurations and specifications were used. During the training of the individual dataset, it was revealed that freezing multiple layers had a counter-productive effect on the overall accuracy of the proposed system. Consequently, the number of freeze layers were kept to zero. For some applications involving learningbased systems, freezing of initial layers has been noted to benefit the overall performance, as it leads to reduction of the overall memory

 Table 2

 Details regarding dataset obtained from different bridges.

Dataset	Bridge Location	Bridge Type	Bridge Dimensions (ft) (length x width)
1	1. Warren County Bridge, NJ	N/A	N/A
2	2. Galena Creek Bridge, NV	Twin Span Arch Bridge	$1726.5 \times 62.0$
	3. East Helena Bridge, MT	Concrete Tee-Beam Bridge	$66.9 \times 40.0$
	4. Kendall Pond Rd Bridge, NH	Girder Bridge	$78.1 \times 44.0$
	5. Piscataqua Bridge, ME	Through-Arch Bridge	4503 × 98
3	6. Broadway Bridge, AR	Arch Bridge	$2786 \times 40$
	7. Fordway Bridge, NH	Beam Bridge	$131 \times 23$
	8. Dove Creek Rd Bridge, BC	Beam Bridge	50 × 45
	9. Baxterville Bridge, CO	Lost-through Truss Bridge	$117 \times 15.4$

Table 4
Accuracy and error for rebar detection system trained using ResNet-34 and dataset 1.

Batch Size	Number of E	A			
	20	40	80	100	Average
4	98.92/3.79	98.67/3.72	98.44/4.16	98.64/3.82	98.67/3.87
8	98.64/4.04	98.67/4.47	98.69/4.33	98.72/4.03	98.68/4.22
16	<b>98.89</b> /2.91	<b>98.89</b> /3.62	<b>98.72</b> /3.79	<b>98.86</b> /3.19	98.84/3.38
32	<b>98.39</b> /4.77	<b>98.69</b> /3.86	<b>98.53</b> /4.02	<b>98.36</b> /4.55	98.49/4.30
Average	98.71/3.88	98.73/3.92	98.60/4.08	98.65/3.90	

**Table 5**Accuracy and error for rebar detection system trained using ResNet-50 and dataset 1.

Batch Size	Number of E	<b>A</b>			
Batch Size	20	40	80	100	Average
4	94.44/	94.72/	94.72/	96.39/	95.07/
	15.48	15.17	17.99	14.38	15.76
8	95.28/	96.39/9.68	95.83/	97.50/9.66	96.25/
	13.17		11.22		10.92
16	97.50/8.37	<b>96.39</b> /8.79	<b>95.28</b> /9.79	<b>96.39</b> /9.16	96.39/9.03
32	98.33/6.72	95.28/	97.78/8.18	95.56/	96.74/9.60
		12.02		11.46	
Average	98.39/	95.70/	95.90/	96.46/	
	10.94	11.42	11.80	11.17	

utilization and hastens the training process.

Table 4-7 highlights the performance of dataset 1 for the different ResNet architectures (i.e. ResNet-34, ResNet-50, ResNet-101, ResNet-152), which vary in terms of their depth, number of epochs and batch sizes of the trained network architecture. The purpose of this evaluation is to examine the effect of number of layers on the overall performance on the rebar detection system. For majority of instances given in Table 4-7, increase in batch size results in improved training performance of the rebar detection systems. However, in some of the cases, the accuracy of the system trained for batch size equal to 32 is slightly lower than systems trained with batch size equal to 16. Similarly, for majority the of cases of system training with different network parameters (i.e. batch size and number of there is increase in the overall accuracy and decrease in the loss/error value of the trained rebar detection system.

Similar to the results highlighted for dataset 1, in Table 8-11, the details regarding the accuracy and loss of the different ResNet architectures trained for dataset 2 have been outlined. It can be seen in Table 8-11 that for majority of instances, an increase in the batch size resulted in improved accuracy and decreased system loss/error rate of the trained rebar detection systems. There are some instances in which the results with the highest accuracy do not necessarily correspond to systems with the highest batch size. In order to facilitate the

**Table 6**Accuracy and error for rebar detection system trained using ResNet-101 and dataset 1.

Batch Size	Number of E	<b>A</b>			
	20	40	80	100	Average
4	94.72/	97.78/7.11	96.39/	97.78/5.07	96.67/9.95
8	17.04 96.11/8.36	98.33/6.56	10.56 <b>98.33</b> /5.20	<b>98.33</b> /3.95	97.76/6.02
16	97.78/8.82	98.61/4.37	98.61/4.44	<b>98.06</b> /5.11	98.27/5.69
32	98.89/5.52	99.17/3.51	98.89/7.20	99.44/2.33	99.10/4.64
Average	96.86/	98.47/5.39	98.06/6.85	98.40/4.12	
	9.94				

**Table 7**Accuracy and error for rebar detection system trained using ResNet-152 and dataset 1.

Batch Size	Number of E <sub>I</sub>				
	20	40	80	100	Average
4	95.56/ 14.96	97.22/7.23	98.33/8.55	98.06/5.92	97.30/9.17
8	98.33/5.55	97.50/6.04	<b>98.61</b> /6.12	<b>98.89</b> /4.39	98.33/5.53
16	<b>98.61</b> /4.98	<b>98.89</b> /4.51	<b>97.50</b> /5.58	<b>98.61</b> /3.39	98.40/4.62
32	<b>98.06</b> /7.13	<b>97.78</b> /8.14	98.89/2.52	99.72/1.71	98.61/4.88
Average	97.64/8.16	97.85/6.48	98.33/5.69	98.82/3.85	

**Table 8**Accuracy and error for rebar detection system using ResNet-34 and dataset 2.

Batch Size	Number of Epochs				
	20	40	80	100	Average
4	98.50/4.15	98.73/3.63	<b>98.65</b> /3.65	98.42/4.19	98.56/3.91
8	98.72/3.64	98.75/3.48	<b>98.61</b> /3.57	98.66/3.63	98.69/3.58
16	<b>98.89</b> /3.17	98.95/3.16	98.73/3.36	98.74/3.43	98.83/3.28
32	<b>98.77</b> /3.16	98.95/3.06	98.77/3.37	98.86/3.45	98.84/3.26
Average	98.72/3.53	98.85/3.33	98.69/3.49	98.67/3.68	

**Table 9** Accuracy and error for rebar detection system using ResNet-50 and dataset 2.

Batch Size	Number of E	<b>A</b>			
	20	40	80	100	Average
4	97.12/6.57	97.88/6.28	98.03/5.84	97.72/6.56	97.69/6.31
8	<b>98.18</b> /5.12	98.94/4.45	97.57/5.37	98.03/4.96	98.18/4.96
16	<b>97.72</b> /5.49	<b>98.03</b> /5.29	<b>98.63</b> /5.49	98.18/6.15	98.14/5.61
32	97.88/5.23	<b>96.97</b> /9.93	<b>98.48</b> /3.33	99.39/2.36	98.18/5.21
Average	97.73/5.60	97.96/6.49	98.18/5.01	98.33/5.01	

**Table 10**Accuracy and error for rebar detection system using ResNet-101 and dataset 2.

Batch Size	Number of E				
	20	40	80	100	Average
4	97.42/ 10.63	99.09/4.21	97.88/6.32	97.42/ 10.51	97.95/7.91
8	97.72/5.12	<b>98.48</b> /3.84	98.48/3.83	98.48/5.05	98.29/4.50
16	98.33/5.38	<b>98.18</b> /4.13	<b>98.48</b> /4.76	<b>98.33</b> /4.74	98.33/4.75
32 Average	98.33/4.85 <b>97.95/6.49</b>	97.72/5.25 98.37/4.36	95.57/6.33 97.60/5.31	98.18/6.12 98.10/6.61	97.45/5.64

**Table 11**Accuracy and error for rebar detection system using ResNet-152 and dataset 2.

Batch Size	Number of E				
	20	40	80	100	Average
4	98.63/6.14	97.78/7.11	98.03/4.79	98.03/4.94	98.12/5.75
8	98.48/3.96	98.94/4.27	97.88/4.18	97.72/5.91	98.26/4.58
16	98.48/4.97	<b>98.94</b> /3.26	<b>98.48</b> /4.49	<b>99.09</b> /2.97	98.75/3.92
32	98.94/4.33	<b>98.33</b> /4.30	<b>98.33</b> /4.58	<b>97.88</b> /5.78	98.37/4.75
Average	98.63/4.85	98.50/4.74	98.18/4.51	98.18/4.90	

examination of the results for rebar detection system, the average values for each instance of batch size and number of epochs has been calculated. It can be seen from Tables 8 and 9 that increase in batch size leads to increase in accuracy of the rebar detection system. However, there are some examples in which increase in batch size does not

necessarily lead to corresponding increase in the accuracy and decrease in system loss/error rate.

In the following discussion, the focus will shift towards the other metrics that have been used to evaluate the proposed model, which include computational considerations in terms of time taken towards training of the rebar detection system. At the same time, there is also a need to examine the effect of CPU and GPU on the overall training time. Although, the system is trained offline in both instances. However, it is important to consider the training time for real-time systems, as there will be a need for the system to be regularly updated right after data collection from different bridges, which can allow the rebar detection and.

localization system to improve its performance and robustness to different bridges. The earlier discussion regarding accuracy/loss provide information regarding the specific network parameters that lead to the optimal performance of the rebar detection system. In this discussion, the time constraint will be added to the overall discussion, which will provide a balance and compromise between improved robustness, accuracy and reduced computational constraints, as this system has to be practically implemented on an actual robotic platform with limited computational and memory resources, which need to be effectively utilized to ensure that the robot is able to perform localization, mapping, navigation, collision and obstacle avoidance, and various sensorbased operations for data collection in real-time. The details of the performance of the different ResNet architecture networks have been given in Fig. 6-8. Figs. 6 and 7 show bar-plot with average, maximum and minimum values for the different Deep Residual networks. It can be seen from Fig. 6(a) and 6(b) that the average accuracy of ResNet frameworks increases with number of epochs and batch sizes. The increase is steady and varies from one network architecture to another. Similar results are revealed for findings in Fig. 7(a) and Fig. 7(b). Overall, the increase in the number of epochs lead to increase in the accuracy of the rebar detection systems.

It is important to understand that Increase in batch size and number of epochs for system training has different effect on the different network architectures. For example, ResNet-18 highlights very minimal changes in the overall accuracy with increase in batch sizes and number of epochs. It can be concluded from Figs. 6.

and 7 that there is a positive correlation between number of layers and performance of rebar detection method, which is measured here using accuracy and loss metrics. However, in comparison to the effect of number of layers on system accuracy, the effects of batch size and number of epochs on accuracy is not clear for some of the network architectures examined. There is also a need to assess the effect of training time on the number of layers in the network architectures, which are trained using different computational resources. Fig. 8(a) and

Fig. 8(b) examine the change in the training time for the different network architectures trained using CPU and GPU resources respectively. The specification for system labelled as CPU are given as follows: Ubuntu 16.04 LTS, 32 GB memory, 350 GB hard disk, Intel ° Core i7-8700 CPU with 3.2 GHz clock speed. Meanwhile, the system labelled as GPU had the following hardware and software specifications: Ubuntu 18.04 LTS, 32 GB memory, 350 GB hard disk, Intel ° Core i7-8700 CPU with 3.2 GHz clock speed and NVIDIA® GeForce® GTX 1080 TI Graphical Processing Unit (GPU). In Fig. 8(a) and 8(b), the training time has been specified in minutes. It can be seen from Fig. 8(a) that increasing number of layers by a small fraction leads to greater increase in training for the different ResNet frameworks, especially when training using CPU alone. The training time increases from less than 1000 min for ResNet-18 to approximately 5000 min for ResNet-152 architecture, which is a roughly five times increase in the training time. In comparison with these results, it can be seen that the system trained on GPU take significantly reduced time for training and there is a marginal increase in the training time with corresponding increase in the number of layers of the networked architecture. There is a wide difference in training time between CPU and GPU for the different layered architectures, which is evident from cross-examination of Fig. 8(a) and 8(b).

Table 12 outlines the final results for the rebar detection system, which shows the system training using the most promising system training configuration, based on the results obtained in the previous sections. Consequently, each of the system is trained with batch size of 32 and number of epochs equal to 100. In the final evaluation of the rebar detection system, the total dataset containing data from nine bridges is divided into six bridges for testing and three bridges for validation of the system training. The overall performance is examined using training accuracy, training loss, validation accuracy, validation loss and training time. It can be seen in Table 12 that increase in the number of layers of network architecture improves the overall capabilities of the system to accurately detect rebar images from bridges that have not been previously been encountered by the rebar detection system. Comparison of ResNet and DenseNet architectures and their performance given in Tables 1 and 12 respectively reveal that ResNet-152 contains an increased number of parameters, but provides better performance than Densenet-161 in terms of training time, validation accuracy, training accuracy, validation loss and training loss. These results are comparable to the state-of-the-art in the rebar detection systems [48] [68] [69] [70] [71].

#### 4.3. Rebar localization method

In this section, the performance of the rebar localization system will

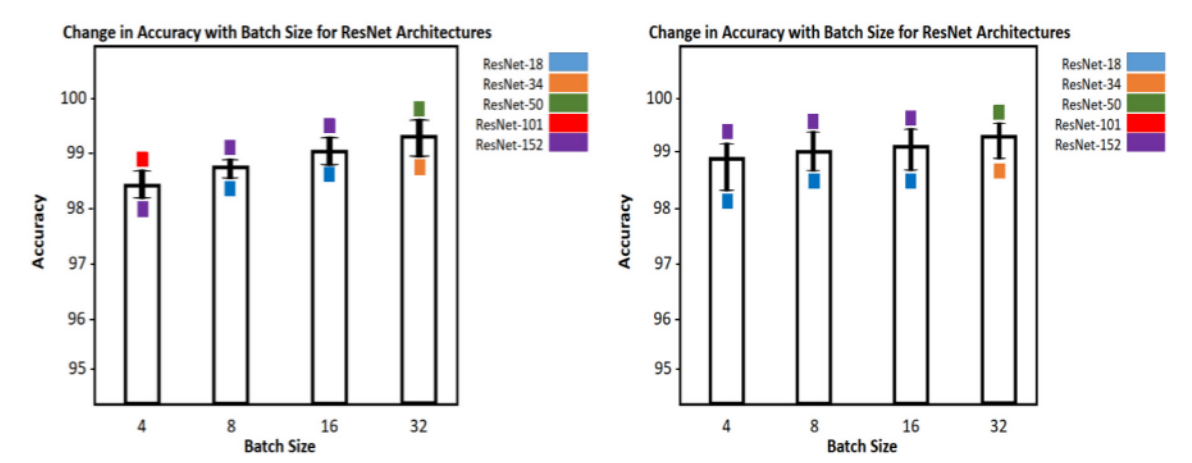


Fig. 6. Result from dataset 3 providing information regarding change in accuracy with constant batch sizes and (a). number of epoch = 20, and (b) number of epoch = 100.

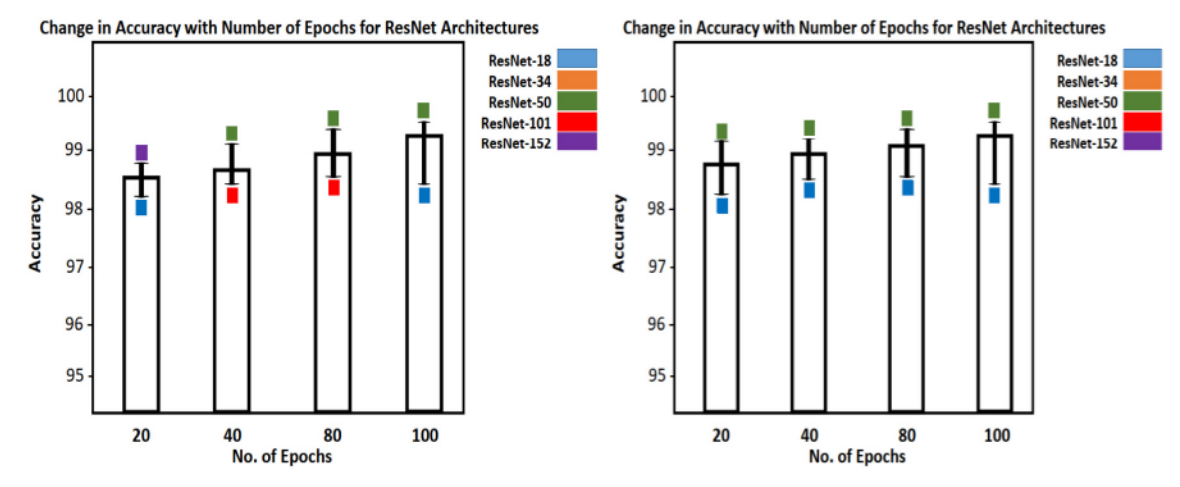


Fig. 7. Result from dataset 3 providing information regarding change in accuracy with constant number of epoch and (a), batch size = 4, and (b) batch size = 32.

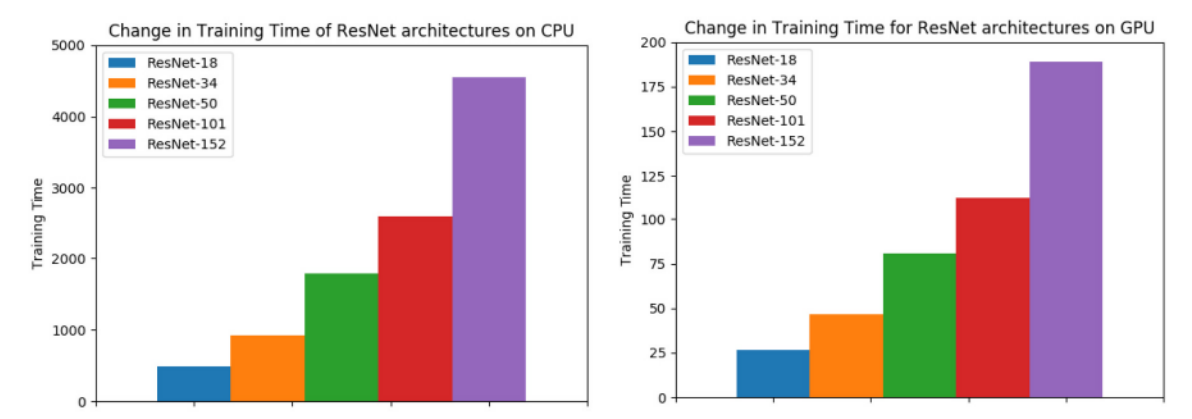


Fig. 8. The results for dataset 3 provide information regarding training time with respect to the number of layers for which the system is being trained for the case of CPU, and GPU.

Table 12

Performance of rebar detection system for different network architectures with results for training and validation.

Network architecture	Training Accuracy	Training Loss	Validation Accuracy	Validation Loss	Train Time (minutes)
ResNet-18	99.23	2.15	80.60	10.2	25
ResNet-34	99.31	2.03	84.70	8.51	47
ResNet-50	99.37	1.66	93.20	7.44	75
ResNet-101	99.37	1.69	94.30	7.05	118
DesneNet-121	99.23	2.00	96.67	18.9	273
ResNet-152	99.42	1.51	97.20	5.32	190
DenseNet-161	99.30	1.89	97.19	11.2	622

be discussed. The majority of studies developed for rebar detection and localization in the past have not emphasized on the exploration of the performance from a multi-dimensional perspective. In contrast to those studies, this research will ensure that the performance of the proposed rebar detection and localization system is assessed using a wide-range of available techniques for performance evaluation. The discussion of the results for rebar localization will be divided into two sections, namely the qualitative and quantitative analyses. In the qualitative analysis section, the focus will be towards examining the qualitative aspects of the results, which pertain to the visual evaluation of the way in which the rebar localization process has taken place, along with the difficulties faced towards the accurate localization of the individual rebar images. There are various factors that affect the accurate localization of the rebar profiles; these factors will be discussed in terms of the ways in which data from different bridge was affected with these different factors. A visual appraisal of these factors will provide insights that will enable the improvement of the different processes underlying rebar localization. For the quantitative analysis of the results, there will be a need to examine the performance of the proposed rebar localization using different statistical measures.

#### 4.3.1. Qualitative analysis

The qualitative analysis for rebar localization system deals with the examination of the results obtained using the human visual system in terms of accuracy and the overall quality of rebar localization using the system proposed in this study. As, the name suggests, the qualitative analysis can vary from one subjective viewer to another. It is for this reason that civil experts (i.e. someone with a level of familiarity and experience with the use of GPR sensor for civil infrastructures and detection of sub-surface objects using GPR data) are required for effectively highlighting the rebar signatures within GPR images and assessing their overall accuracy towards rebar localization in GPR images. Fig. 9 outlines results for rebar localization from different dataset using green bounding boxes within GPR images (Fig. 2 and Fig. 9 provide

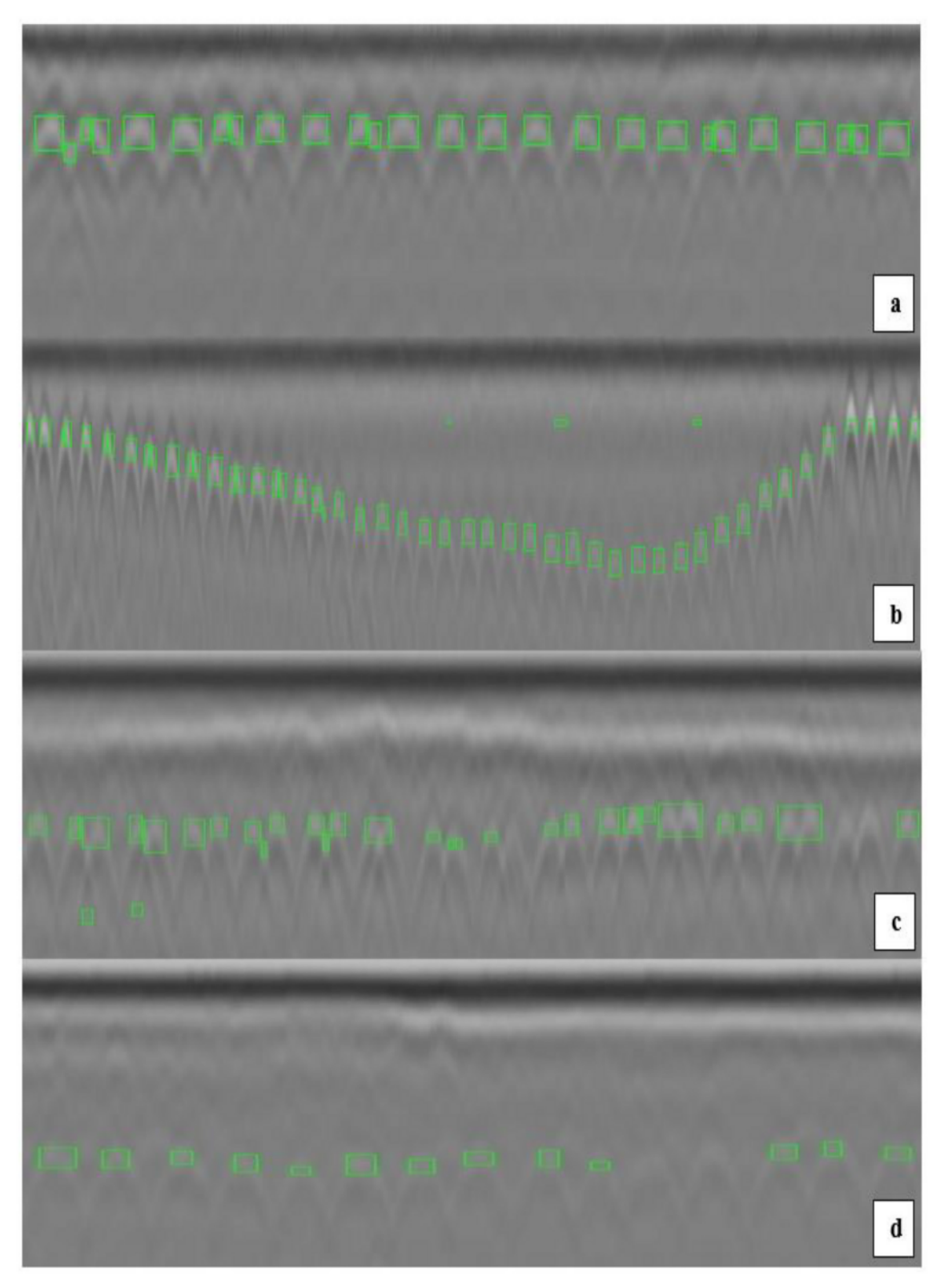


Fig. 9. The result for rebar localization for bridges with different levels of difficulty in rebar recognition: (a) Warren County, NJ bridge in dataset 1, (b) East Helena bridge, which belongs to dataset 2 (c) data from Dove Creek Bridge, (d) data from Fordway Bridge.

GPR data from different bridges in different order). The GPR scan images in Fig. 9 are small portions of the overall GPR scan.

data obtained from different bridges. It can be seen that each of the dataset from the different bridges contain varying levels of noise, reflection signals and other non-rebar artefacts. For the case of Fig. 9(a), which contains GPR image from dataset 1 (i.e. Warren County, NJ

bridge) with limited amount of noise leading to effective rebar detection and localization. Similar findings are revealed for Fig. 9(b) containing GPR image from dataset 2 leading to accurate localization of rebar signatures.

Conversely, for the case of bridge dataset from Dove Creek bridge and Fordway bridge, which are given in Fig. 9(c) and 9(d) respectively,

**Table 13**Confusion Matrix for rebar localization using dataset 1.

		Predicted Results		
Actual Results	Class No Rebar Class Rebar	Class No Rebar TN = 0% FN = 0.98%	Class Rebar FP = 1.48% TP = 97.50%	

**Table 14**Confusion Matrix for rebar localization using dataset 2.

		Predicted Results		
Actual Results	Class No Rebar Class Rebar	Class No Rebar TN = 0% FN = 0.67%	Class Rebar FP = 4.25% TP = 95.30%	

**Table 15**Confusion Matrix for rebar localization using dataset 3.

		Predicted Results		
Actual Results	Class No Rebar Class Rebar	Class No Rebar TN = 0% FN = 6.83%	Class Rebar FP = 10.23% TP = 82.93%	

there is a considerable level of noise and reflection artefacts, which prevented the successful recognition and localization of different rebar signatures. At the same time, there is some misclassification of reflective signals and artefacts as correct rebar signatures. There are reflective signals in the shape of parabolic shapes that are depicted above and below the actual rebar profiles, which has led to the false classification of some of these reflective signals as actual rebar signatures. Due to the noise-related artefacts in the GPR data, there are some instances of false negative (the actual rebar profiles that are not accurately detected) and false positive (noise and other artefacts that are wrongly classified as rebar profile) within the dataset 3. In contrast to the dataset 1 and 2, the GPR data for bridges in dataset 3 contain considerable level of noise, and reflective artefacts, which leads to difficulties in the accurate localization of the rebar signals. These types of anomalous artefacts are not present in GPR data from dataset 1 and 2.

#### 4.3.2. Quantitative analysis

The quantitative analysis deals with the statistical aspect of the performance related to the rebar localization system developed in this study. A number of different performance evaluation metrics are used in the relevant literature for the effective examination of system performance. Tables 13-15 outline the results in the form of confusion matrix for the rebar localization for dataset 1, 2 and 3 respectively. The values in the confusion matrices for TP (True Positive), FP (False Positive), TN (True Negative), and FN (False Negative) are given in the

form of percentages. The confusion matrices for the different dataset highlight the variation for the two classes (i.e. rebar and non-rebar classes) between the actual values of the images and the predicted values that were reported by the proposed rebar localization method. Since, the primary purpose of the rebar localization algorithm is to separate rebar signatures, it is for this reason that the TP values are equal to zero, as the rebar localization is not used to high non-rebar regions, but to separately highlight rebar regions only. It can be seen from the results in Tables 13-15 that the proposed rebar localization technique has provided a high level of accuracy, due to which, this system can be implemented in a practical NDE system for infrastructure monitoring and assessment. For the calculation of the different statistical properties related to performance evaluation, a number of different mathematical formulas have been used. The mathematical detail for the different statistical criteria have been outlined in eq. 4-9, which are given below:

$$Accuracy = \frac{(TP + TN)}{(TP + TN + FP + FN)} \tag{4}$$

Error Rate = 
$$\frac{FP + FN}{(TP + FP + TN + FN)}$$
 (5)

$$Recall = \frac{TP}{(TP + FP)}$$
 (6)

$$Precision = \frac{TP}{(TP + FN)}$$
 (7)

$$F1 - score = 2 \times \frac{(Precision \times Recall)}{(Precision + Recall)}$$
(8)

$$IoU = \frac{(Area_{Ground} \cap Area_{Output})}{(Area_{Ground} \cup Area_{Output})}$$
(9)

The statistical criteria for performance evaluation outlined in eq. (4)–(8) have been adopted from [110]. Table 16 outlines the comparison between the performance of the proposed method in this research with state-of-the-art for rebar localization methods in relation to the different performance evaluation metrics [48,68,70,71,111,112]. This shows that majority of the studies on rebar localization do not put enough emphasis on the statistical evaluation of the performance of the proposed rebar localization. Unlike prior studies, this research has leveraged different statistical performance evaluation metrics that are widely employed in the field of machine learning. The performance of the rebar localization system is comparable or superior to the different algorithms discussed in the state-of-the-art. Fig. 10 highlights the process for calculating Intersection-over-Union (IoU) given in eq. (9), which has gained importance in recent years in order to cater to class imbalances within classification problems.

Table 16

Quantitative performance evaluation of the rebar localization system and comparison with recent studies (red region shows metrics not highlighted in studies).

Study	Accuracy	Error	Precision	Recall	F1-score	IoU	Time
Dou <b>[111]</b>			70.04%	70.80%	70.20%		730 ms
Kaur <b>[48]</b>	91.98%						
Gibb <b>[68]</b>	95.05%						
Dinh <b>[71]</b>	99.60%						
Ahmed <b>[70]</b>	94.52%		95.18%				
Harkat <b>[112]</b>	88.99%						
This study	91.91%	8.14%	96.89%	94.41%	95.58%	90.20%	372 ms

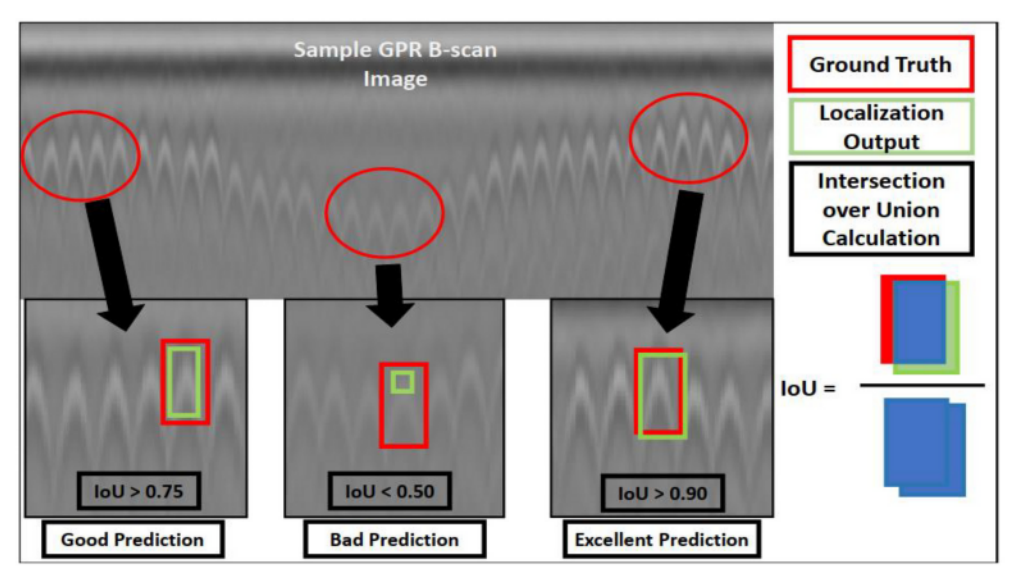


Fig. 10. An illustration to highlight calculation of Intersection over Union (IoU) with examples to highlight the difference between suitable and unsuitable instances.

Table 17
The effects of different factors for the GPR data acquired from the different bridges in this research.

		Factors Affecting Performance for different bridge data				
Datase t	Bridge Location	Inter- Signature Separation	Rebar Signature Brightness	Reflections	Noise	
1	1. Warren County, NJ	High	High	Low	Low	
2	2. Galena Creek Bridge, NV	Low	Moderate	Moderate	Moderate	
	3. East Helena Bridge, MT	Moderate	High	Moderate	Moderate	
	4. Kendall Pond Road Bridge, NH	Low	Low	Low	Moderate	
	5. Piscataqua Bridge, ME	Low	Moderate	Moderate	Moderate	
3	6. Broadway Bridge, AR	Low	Low	Moderate	Moderate	
	7. Fordway Bridge, Derry, NH	Low	Moderate	High	High	
	8. Dove Creek Bridge, BC	Moderate	Low	Moderate	Moderate	
	9. Baxterville Bridge, CO	Low	Low	Moderate	Moderate	

#### 5. Discussion

In this section, the prime focus of the discussion will be towards examining practical issues within the different processes for rebar detection and localization,

affect the overall performance of the rebar detection and localization system. One of the main issues is data collection. Due to the different bridge physical properties and the environmental conditions during the data collection process, the quality of data can vary drastically. It is for this reason that robustness is essential for improved performance of rebar detection system, which can be increased by incorporating data from multiple bridges. However, there are various noise artefacts and reflection signals within the GPR images, which are similar to actual rebar signatures. The different anomalous features, (various noise artefacts that cause cluttering and reduce the variation between foreground and background, reflection signals that mimic parabolic rebar signatures, and level of overlap between the adjacent rebar profiles) are outlined in Fig. 10. The differentiation of these noise artefacts and reflection signals from the actual rebar signatures can pose significant challenges towards accuracy of the proposed rebar detection system. There is also an element of human-error in relation to the development of database for the rebar detection towards differentiating between rebar and non-rebar elements in the different GPR images. Another challenge for the development of rebar detection system relates to the inherent limitations of the type of learning algorithm used for classifying rebar and non-rebar images from the original GPR data.

The first issue that can jeopardize the accuracy of the rebar localization relates to the robustness of the rebar detection system towards handling data from different bridges. The block-based sliding window approach towards rebar localization also has some drawbacks, which can affect its overall performance. For a sliding window of fixed size, it can be difficult to accurately localize rebar signatures within the rebar detection and localization systems in real-world scenarios. Table 17 outlines the data collected from different bridges and the effect of the different factors towards reducing the overall effectiveness of the proposed rebar detection and localization method. The different factors that can potentially impact the overall performance of the rebar detection and localization system include the following:

(i). Reflections in GPR images: The parts of the GPR image that contain parabolic.

reflective anomalies, which are visually similar to the actual rebar signatures. The frequency of occurrence of these reflection decreases the overall performance of the rebar detection and localization system, which is one of the reasons for the lower performance of the proposed localization method on dataset 3. It can be seen that Fig. 11(a) contains a higher frequency of such reflections at the lower-end of the GPR image, followed by reduced level of reflections in Fig. 11(c) at the upper-end of the GPR image. There is a lower presence of reflection observed in Figs. 11(b) and 11(d).

(ii). Inter-signature separation: Another important factor is the level of visual separation between the adjacent rebar signatures, which can

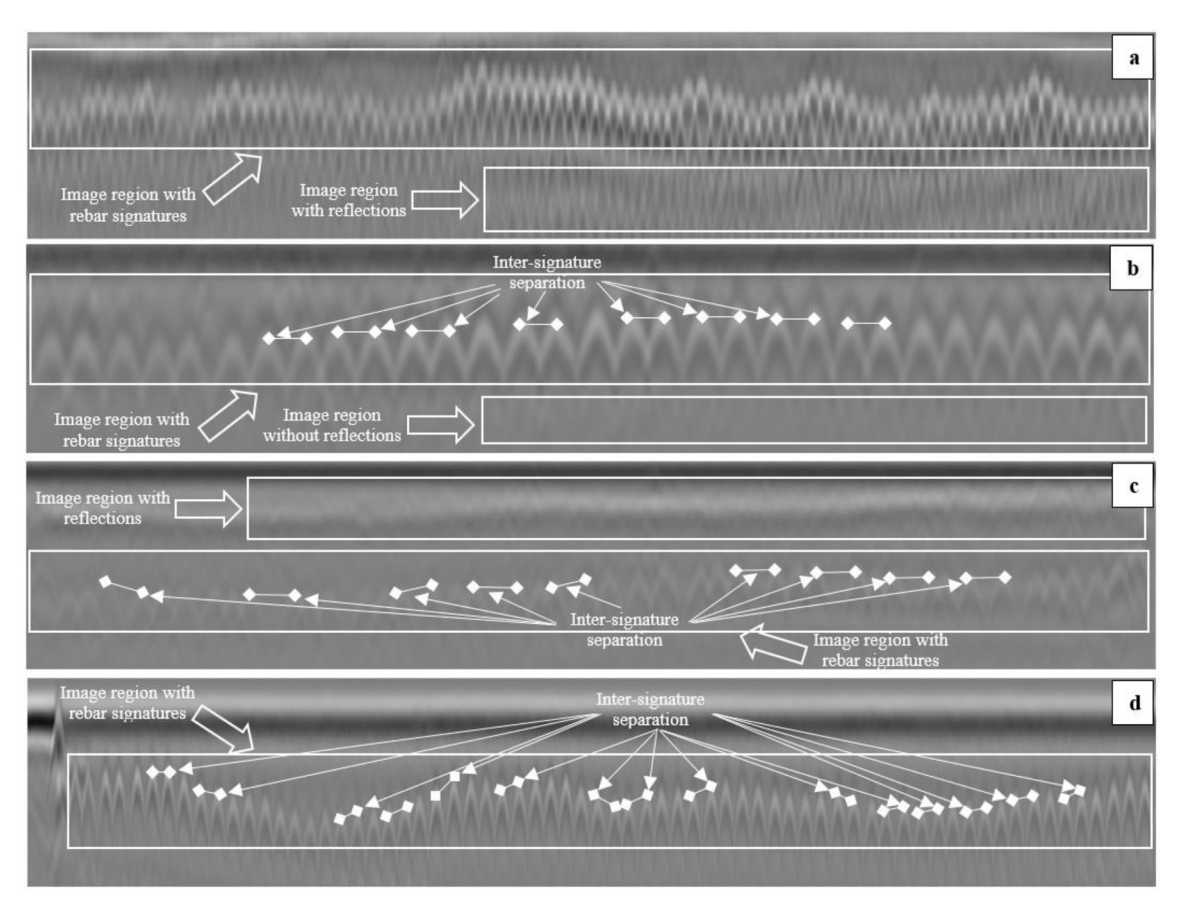


Fig. 11. Some of the factors affecting the performance of rebar detection and localization algorithm for the following bridges: (a) data from Fordway bridge, (b) Warren County Bridge, (c) Dove Creek bridge, and (d) East Helena Bridge.

affect the performance of the rebar detection and localization system. The greater the inter- signature separation, the better the ability of the rebar detection and localization system towards detecting and localizing the individual rebar signatures. Conversely, reduced inter-signature separation leads to increased overlapping between adjacent rebar signatures such that it becomes increasingly challenging for the rebar detection and localization system to separately detect and localize each parabolic signature. It can be seen in Fig. 11(a) that the intersignature separation is very low. However, for the case of Figs. 11(b), 11(c) and 11(d), it can be seen that the inter- signature separation is high, which leads to improved performance of rebar detection and localization system.

(iii) Rebar signature brightness The overall performance of the proposed rebar detection and localization system is dependent on its ability to effectively differentiate between the foreground and background regions. This process can be facilitated due to the distinct visual properties (e.g. brightness, parabolic shape and difference in the visual elements between foreground and background regions) of the rebar signatures. The overall brightness of the rebar profiles in Figs. 11(a), 11(b) and 11(d) is sufficient to allow effective differentiation between foreground and background regions. For the case of Fig. 11(b), the reduced brightness of rebar signatures leads to increased challenges for rebar detection and localization system.

(v). Noise: The effect of noise can manifest within GPR images in a number of different ways. Increased overlapping between adjacent rebar signatures can lead to noise between the overlapping rebar signatures, which makes it challenging to separately identify the individual rebar signatures. There can also be blurring effect in the different segments of the GPR image, which can reduce the performance of rebar detection and localization system.

#### 6. Conclusion and future works

This paper has discussed the development of rebar detection and localization system, which is based on different supervised (Deep Residual Networks) and unsupervised (K-means clustering) learningbased techniques. This method has been tested and evaluated using novel dataset collected from real bridges that has not been used in any of the existing studies. This research provides an examination of the research problem with focus towards utilizing Deep Learning frameworks, in particular the Deep Residual Networks (ResNets) and Deep Dense Networks (DenseNets). A wide-range of performance evaluation metrics were leveraged for the rebar detection and localization system, which can provide insights towards developing a robust, real-time practical rebar detection and localization system for bridge inspection and monitoring. A comparison of proposed method for rebar detection and localization with recent research revealed that performance of the proposed system is better or at par with state-of-the-art. A number of different factors have also been identified, which affect the overall performance of the rebar detection and localization systems.

There are various existing deficiencies in this research area, which should be improved by the future researchers in this field. These issues have been highlighted in the discussion section. There is a need to develop rebar detection and localization systems that are able to better differentiate between the noise/reflection artefacts (reflection artefacts have the property of being similar in visual characteristics to the actual parabolic rebar profiles) and actual rebar signatures within GPR data. There is also a need to include data from additional bridges for development of practical, robust and reliable rebar detection and localization systems. In order to further improve on the state-of-the-art, future researchers should develop real-time rebar detection and localization systems that provide reliable performance that can be deployed within

efficient, real-time bridge inspection robots in the future.

#### **Declaration of Competing Interest**

The authors declare that they have no known competing financial interests or personal relationships that could have appeared to influence the work reported in this paper.

#### Acknowledgment

This work is supported by the U.S. National Science Foundation (NSF), USA under grants NSF-CAREER 1846513 and NSF-PFI-TT 1919127, and the U.S. Department of Transportation, Office of the Assistant Secretary for Research and Technology (USDOT/OST-R), USA under Grant No. 69A3551747126 through INSPIRE University Transportation Center. This research is also supported by Vingroup Innovation Foundation (VINIF), Vietnam in project code VINIF.2020.NCUD.DA094. The views, opinions, findings and conclusions reflected in this publication are solely those of the authors and do not represent the official policy or position of the NSF, the USDOT/OST-R and other entities.

#### References

- [1] A. Penn, The deadliest bridge collapses in the US in the last 50 years, CNN, 15 March 2018. [Online], Retrieved from: https://www.cnn.com/2018/03/15/us/bridge-collapse-history-trnd/index.html [Accessed on 20 June 2020].
- [2] R.S. Kirk, W.J. Mallett, Highway Bridge Conditions: Issues for Congress, Washington, DC: US Congressional Research Service, R44459. 2013. [Online], Retrieved from: https://crsreports.congress.gov/product/pdf/R/R44459/8.
- [3] L. Wright, P. Chinowky, K. Strzepek, R. Jones, R. Streeter, J.B. Smith, J.-M. Mayotte, A. Powell, L. Jantarasami, W. Perkins, Estimated effect of climate change on flood vulnerability of US bridges, Mitigation Adaptation Strategies Global Change 17 (8) (2012) 939–955, https://doi.org/10.1007/s11027-011-9354-2 [Accessed on 10 March 2020].
- [4] J.-L. Briaud, L. Brandimarte, J. Wang, Probability of scour depth exceedance owing to hydrologic uncertainty, Georisk 2 (77–88) (2014) 1, https://doi.org/10. 1080/17499510701398844 [Accessed on 11 March 2020].
- [5] U.S. Department. of Transportation Report, Status of the Nation's Highways, Bridges, and Transit: Conditions and Performance, Washington, DC: US Department of Transportation, 2010. [Online], Retrieved from: https://www.fhwa.dot.gov/policy/2010cpr/pdfs/cp2010.pdf.
- [6] W. Cook, P.J. Barr, M.W. Haling, Bridge failure rate, J. Perform. Constr. Facil. 29 (3) (2015) 1–8, https://doi.org/10.1061/(asce)cf.1943-5509.0000571 [Accessed on 21 March 2020].
- [7] J. Neumann, J. Price, P. Chinowsky, L. Wright, L. Ludwig, R. Streeter, R. Jones, J. B. Smith, W. Perkins, L. Jantarasami, et al. Climate change risks to US infrastructure: impacts on roads, bridges, coastal development and urban drainage Climate Change, 131, 1, pp. 97–109. DOI: https://doi.org/10.1007/s10584-013-1037-4. [Accessed on 02 April 2020].
- [8] H.M. La, N. Gucunski, K. Dana, S.H. Kee, Development of an autonomous bridge deck inspection robotic system, Journal of Field Robotics 34 (8) (2017) 1489–1504, https://doi.org/10.1002/rob.21725 [Accessed on 10 April 2020].
- [9] G. C. Lee, S. B. Mohan, C. Huang and B. N. Fard, A Study of Bridge Failures (1980–2012), Buffalo, NY: The State University of New York. ISBN: 1520-295X. [Accessed on 01 February 2020].
- [10] M.M. Flint, O. Fringer, S.L. Billington, D. Freyberg, N.S. Diffenbaugh, Historical analysis of hydraulic bridge collapses in the continental United States, J. Infrastruct. Syst. 23 (3) (2017) 1–16, https://doi.org/10.1061/(asce)is.1943-555x 0000354 [Accessed on 10 March 2020].
- [11] A. Khelifa, L. A. Garrow, M. J. Higgins and M. D. Meyer, Impact of climate change on scour-vulnerable bridges: assessment based on HYRISK, J. Infrastruct. Syst., vol. 19, no. 2, pp. 138–146, 2013. DOI: https://doi.org/10.1061/(asce)is.1943-555x.0000109. [Accessed on 11 February 2020].
- [12] N. Gucunski, S. H. Kee, H. M. La, B. Basily and A. Maher, Delamination and concrete quality assessment of concrete bridge decks using a fully autonomous RABIT platform International Journal of Structural Monitoring and Maintenance, vol. 2, no. 1, pp. 19–34, 2015. DOI: 10.12989/smm.2015.2.1.019. [Accessed on 01 March 2020].
- [13] H. Ahmed, H.M. La, N. Gucunski, Review of non-destructive infrastructure evaluation of bridges: state-of-the-art robotic platforms, sensors and algorithms, Sensors. Special Issue on Innovative Sensors for Civil Infrastructure Condition Assessment. 20 (14) (2020) 1–38 ISSN 1424-8220 [Accessed on 03 July 2020].
- [14] P. Prasanna, K. Dana, N. Gucunski, B. Basily, H.M. La, R.S. Lim, H. Parvardeh, Automated crack detection on concrete bridges, IEEE Trans. Autom. Sci. Eng. 13 (2) (2016) 591–599, https://doi.org/10.1109/tase.2014.2354314 [Accessed on 01 February 2020].
- [15] H.M. La, N. Gucunski, S.-K. Kee, J. Yi, T. Senlet, L. Nguyen, autonomous robotic

- system for bridge deck data collection and analysis, in: proceedings of IEEE international conference on intelligent robots and Systems (IROS), Chicago, IL, USA 14-18 (Sept. 2014) 1950–1955, https://doi.org/10.1109/IROS.2014.6942821 [Accessed on 11 March 2020].
- [16] H.M. La, R.S. Lim, B. Basily, N. Gucunski, J. Yi, A. Maher, F.A. Romero, H. Parvardeh, autonomous robotic system for high-efficiency non-destructive bridge deck inspection and evaluation, proceedings of IEEE international conference on automation science and engineering (CASE), Madison, WI, USA 17-21 (Aug. 2013) 1053–1058, https://doi.org/10.1109/CoASE.2013.6653886 [Accessed on 12 May 2020].
- [17] T. Le, S. Gibb, N. Pham, H. M. La, L. Falk and T. Berendsen, Autonomous Robotic System using Non-Destructive Evaluation methods for Bridge Deck Inspection In: Proceedings of IEEE International Conference on Robotics and Automation (ICRA), Singapore, Singapore, May 29–June 3 2017; pp. 3672–3677. DOI: https://doi.org/ 10.1109/ICRA.2017.7989421. [Accessed on 17 March 2020].
- [18] A. Sirken, G. Knizhnik, J. McWilliams, S. Bergbreiter, BRIDGE risk investigation diagnostic grouped exploratory (BRIDGE) bot, proceedings of IEEE international conference on intelligent robots and Systems (IROS), Vancouver, Canada 24-28 (Sept. 2017) 6526–6532, https://doi.org/10.1109/IROS.2017.8206562 [Accessed on 04 February 2020].
- [19] N. Pham, H.M. La, design and implementation of an autonomous robot for steel bridge inspection, in: proceedings of annual Allerton conference, Monticello, IL, USA 27-30 (Sept. 2016) 556–562, https://doi.org/10.1109/ALLERTON.2016. 7852280 [Accessed on 01 February 2020].
- [20] R.S. Lim, H.M. La, Z. Shan, W. Sheng, developing a crack inspection robot for bridge maintenance, proceedings of IEEE/RSJ international conference on robotics and automation, Shanghai, China. 9–13 (May, 2011) 6288–6293, https://doi.org/ 10.1109/ICRA.2011.5980131 [Accessed on 12 February 2020].
- [21] S.T. Nguyen, H.M. La, development of a steel bridge climbing robot, in: proceedings of IEEE international conference on intelligent robots and Systems (IROS), Macau, China 4-8 (Nov. 2019) 1912–1917, https://doi.org/10.1109/IROS40897.2019.8967748 [Accessed on 14 February 2020].
- [22] Z. Zheng, S. Hu, N. Ding, a biologically inspired cable climbing robot: CCRobot-design and implementation, in: proceedings of IEEE international conference on robotics and Biomimetics (ROBIO), Kuala Lumpur, Malaysia 12-15 (Dec. 2018) 2354–2359, https://doi.org/10.1109/ROBIO.2018.8665180 [Accessed on 06 March 2020].
- [23] Z. Zheng, M. Yang, X. Yuan, N. Ding, A Light-Weight Wheel-Based Cable Inspection Climbing Robot: From Simulation to Reality, In: Proceedings of IEEE International Conference on Robotics and Biomimetics (ROBIO), Kuala Lumpur, Malaysia, 12–15 Dec. p. 1365–1370, (2018), https://doi.org/10.1109/ROBIO. 2018.8665062 [Accessed on 01 March 2020].
- [24] R.T. Pack, J.L. Christopher, K. Kawamura, a Rubbertuator-based structureclimbing inspection robot, in: proceedings of IEEE international conference on robotics and automation (ICRA), Washington, DC, USA 11-15 (May 1997) 1869–1874, https://doi.org/10.1109/ROBOT.1997.619060 [Accessed on 13 February 2020].
- [25] Q. Liu, Y. Liu, An Approach for Auto Bridge Inspection Based on Climbing Robot, In: Proceedings of IEEE International Conference on Robotics and Biomimetics (ROBIO), Shenzhen, China, 12–14 Dec. pp. 2581–2586, (2013), https://doi.org/ 10.1109/ROBIO.2013.6739861 [Accessed on 05 February 2020].
- [26] X. Li, C. Gao, Y. Guo, F. He, Y. Shao, Cable surface damage detection in cable-stayed bridges using optical techniques and image mosaicking, Opt. Laser Technol. (2019) 36-43, https://doi.org/10.1016/j.optlastec.2018.07.012 [Accessed on 01 March 2020].
- [27] K.H. Cho, Y.H. Jin, H.M. Kim, H. Moon, J.C. Koo, H.R. Choi, Caterpillar-based cable climbing robot for inspection of suspension bridge hanger rope, in: proceedings of IEEE international conference on automation science and engineering (CASE), Madison, WI, USA 17-21 (Aug. 2013) 1059–1063, https://doi.org/10.1109/CoASE.2013.6653913 [Accessed on 10 February 2020].
- [28] A. Leibbrandt, G. Caprari, U. Angst, R.Y. Siegwart, R.J. Flatt, B. Eisener, Climbing robot for corrosion monitoring of reinforced concrete structures, In: Proceedings of International Conference on Applied Robotics for the Power Industry, Zurich, Switzerland 11-13 (Sept. 2012) 10–15, https://doi.org/10.1109/CARPI.2012. 6473365 [Accessed on 11 February 2020].
- [29] S. T. Nguyen, A. Q. Pham, A. C. Motley and H. M. La, A Practical Climbing Robot for Steel Bridge Inspection, In: Proceedings of the 2020 IEEE International Conference on Robotics and Automation (ICRA), Paris, France, May 31–June 4, 2020. pp. ISBN: 978-1-7281-7395-5. [Accessed on 01 June 2020].
- [30] Z. Zheng, N. Ding, design and implementation of CCRobot-II: a palm-based cable climbing robot for cable-stayed bridge inspection, in: proceedings of IEEE international conference on robotics and automation (ICRA), Montreal, Canada 20-24 (May 2019) 9747–9753, https://doi.org/10.1109/ICRA.2019.8793562 [Accessed on 10 February 2020].
- [31] K. H. Cho, Y. H. Jin, H. M. K. Kim and H. R. Choi, Development of Novel Multifunctional Robotic Crawler for Inspection of Hanger Cables in Suspension Bridges, In: Proceedings of IEEE International Conference on Robotics and Automation (ICRA), Hong Kong, China, 31 May- 5 June 2014. pp. 2673–2678. DOI: https://doi.org/10.1109/ICRA.2014.6907242. [Accessed on 12 February 2020].
- [32] P. Kriengkomol, K. Kamiyama, M. Kojima, M. Horade, Y. Mae, T. Arai, hammering sound analysis for infrastructure inspection by leg robot, in: proceedings of the IEEE conference on robotics and Biomimetics (ROBIO), Harbin, China 7-10 (Aug. 2015) 887–892, https://doi.org/10.1109/ROBIO.2015.7418883 [Accessed on 01 February 2020].
- [33] K.H. Cho, H.M. Kim, Y.H. Jin, F. Liu, H. Moon, J.C. Koo, H.R. Choi, Inspection

- robot for hanger cable of suspension bridge: mechanism design and analysis, IEEE Transactions on Mechatronics 18 (6) (2013) 1665–1674, https://doi.org/10. 1109/TMECH.2013.2280653 [Accessed on 01 March 2020].
- [34] Z. Zheng, X. Yuan, H. Huang, X. Yu, N. Ding, Mechanical Design of a Cable Climbing Robot for Inspection on a Cable-Stayed Bridge, In: Proceedings of World Congress on Intelligent Control and Automation, Changsha, China, 4–8 July. pp. 1680–1684, (2018), https://doi.org/10.1109/WCICA.2018.8630709 [Accessed on 14 February 2020].
- [35] K.H. Cho, Y.H. Jin, H.M. Kim, H. Moon, J.C. Koo, H.R. Choi, Multifunctional robotic crawler for inspection of suspension bridge hanger cables: mechanism design and performance validation, IEEE Transactions on Mechatronics 22 (1) (2017) 236–246, https://doi.org/10.1109/TMECH.2016.2614578 [Accessed on 01 February 2020].
- [36] P. Kriengkomol, K. Kamiyama, M. Kojima, M. Horade, Y. Mae, T. Arai, New tripod walking method for legged inspection robot, Proceedings of International Conference on Mechatronics and Automation, Dali, China 6-8 (Dec. 2016) 1078–1083, https://doi.org/10.1109/ICMA.2016.7558712 [Accessed on 05 February 2020].
- [37] G. Andrikopoulos, A. Papadimitriou, A. Brussell, G. Nikolapoulos, on model-based adhesion control of a vortex climbing robot, in: proceedings of international conference on intelligent robots and Systems (IROS), Macau, China 4-8 (Nov. 2019) 1460–1465, https://doi.org/10.1109/IROS40897.2019.8968069 [Accessed on 05 February 2020].
- [38] H.M. La, R.S. Lim, B. Basily, N. Gucunski, J. Yi, A. Maher, F.A. Romero, H. Parvardeh, Mechatronic and control systems design for an autonomous robotic system for high-efficiency bridge deck inspection and evaluation, IEEE Transactions on Mechatronics 18 (6) (2013) 1655–1664, https://doi.org/10. 1109/TMECH.2013.2279751 [Accessed on 05 February 2020].
- [39] N. Morozovsky, and T. Bewley, SkySweeper: A Low DOF, Dynamic High Wire Robot, In: Proceedings of IEEE International Conference on Intelligent Robots and Systems (IROS), Tokyo, Japan,3–7 Nov. 2013 pp. 2339–2344. DOI: https://doi. org/10.1109/IROS.2013.6696684. [Accessed on 06 February 2020].
- [40] A. Ellenberg, A. Kontsos, F. Moon, I. Bartoli, Bridge deck delamination identification from unmanned aerial vehicle infrared imagery, Autom. Constr. 72 (2016) 155–165, https://doi.org/10.1016/j.autcon.2016.08.024 [Accessed on 03 February 2020].
- [41] R. Xie, J. Yao, K. Liu, X. Lu, Y. Liu, M. Xia, Q. Zeng, Automatic multi-image stitching for concrete bridge inspection by combining point and line features, Autom. Constr. 90 (2018) 265–280, https://doi.org/10.1016/j.autcon.2018.02. 021 [Accessed on 04 February 2020].
- [42] J. Seo, L. Duque, J. Wacker, Drone-enabled bridge inspection methodology and application, Autom. Constr. 94 (2018) 112–126, https://doi.org/10.1016/j. autcon.2018.06.006 [Accessed on 10 March 2020].
- [43] M. Sakuma, Y. Kobayashi, T. Emaru, A.A. Ravankar, Mapping of pier substructure using UAV, In: Proceedings of IEEE International Symposium on System Integration, Sapporo, Japan 13-15 (Dec. 2016) 361–366, https://doi.org/10. 1109/SII.2016.7844025 [Accessed on 15 February 2020].
- [44] K. Asa, Y. Funabora, S. Doki, K. Doki, Measuring position determination for accurate and efficient visual inspection using UAV, In: Proceedings of IEEE International Symposium on System Integration, Taipei, Taiwan 11-14 (Dec. 2017) 188–193, https://doi.org/10.1109/SII.2017.8279210 [Accessed on 02 February 2020].
- [45] S. Abiko, T. Harada, T. Hasegawa, S. Yuta, N. Shimaji, semi-autonomous collision avoidance flight using two dimensional laser range finder with mirrors for bridge inspection, in: proceedings of IEEE international conference on robotics and Biomimetics (ROBIO), Kuala Lumpur, Malaysia 12-15 (Dec. 2018) 2267–2272, https://doi.org/10.1109/ROBIO.2018.8664780 [Accessed on 06 February 2020].
- [46] B.W. Jiang, C.H. Kuo, K.J. Peng, S.H. Peng, S.H. Hsiung, C.M. Kuo, thrust vectoring control for infrastructure inspection multirotor vehicle, in: proceedings of IEEE international conference on industrial engineering and applications (ICIEA), Tokyo, Japan 26-29 (April 2019) 209–213, https://doi.org/10.1109/IEA.2019. 8714892 [Accessed on 05 February 2020].
- [47] T. Ikeda, S. Yasui, M. Fujihara, K. Ohara, S. Ashizawa, A. Ichikawa, A. Okino, T. Oomichi, T. Fukuda, wall contact by Octo-rotor UAV with one DoF manipulator for bridge inspection, in: proceedings of international conference on intelligent robots and Systems (IROS), Vancouver, Canada 24-28 (Sept. 2017) 5122–5127, https://doi.org/10.1109/IROS.2017.8206398 [Accessed on 07 February 2020].
- [48] P. Kaur, K. Dana, F.A. Romero, N. Gucunski, Automated GPR rebar analysis for robotic bridge deck evaluation, IEEE Transactions on Cybernetics 46 (10) (2016) 2265–2276, https://doi.org/10.1109/tcyb.2015.2474747 [Accessed on 05 February 2020].
- [49] N. Gucunski, B. Basily, J. Kim, J. Yi, T. Doung, K. Dinh, S.-H. Kee, A. Maher, RABIT: implementation, performance validation and integration with other robotic platforms for improved management of bridge decks, International Journal of Intelligent Robotics Applications 1 (2017) 271–286, https://doi.org/10.1007/ s41315-017-0027-5 [Accessed on 03 February 2020].
- [50] C.A. Mueller, T. Fromm, H. Buelow, A. Birk, M. Garsch, N. Gebekken, Robotic bridge inspection within strategic flood evacuation planning in: proceedings of OCEANS 2017, Aberdeen, UK, 19-22 (June 2017), pp. 1–6, https://doi.org/10. 1109/OCEANSE.2017.8084668 [Accessed on 02 February 2020].
- [51] J.E. DeVault, Robotic system for underwater inspection of bridge Piers, IEEE Instrum. Meas. Mag. (2000) 32–37, https://doi.org/10.1109/5289.863909 [Accessed on 01 March 2020].
- [52] R.R. Murphy, E. Steimle, M. Hall, M. Lindemuth, D. Trejo, S. Hurleabaus, Z. Medine-Cetina, D. Slocum, Robot-assisted bridge inspection, J. Intell. Robot. Syst. 64 (2011) 77–95, https://doi.org/10.1007/s10846-010-9514-8 [Accessed on

- 01 February 2020].
- [53] R.S. Lim, H.M. La, W. Sheng, A robotic crack inspection and mapping system for bridge deck maintenance, IEEE Trans. Autom. Sci. Eng. 11 (2) (2014) 367–378, https://doi.org/10.1109/TASE.2013.2294687 [Accessed on 04 February 2020].
- [54] H.M. La, R.S. Lim, B. Basily, N. Gucunski, J. Yi, A. Maher, F.A. Romero, H. Parvardeh, Mechatronic and control systems design for an autonomous robotic system for high-efficiency bridge deck inspection and evaluation, IEEE Transactions on Mechatronics 18 (6) (2013) 1655–1664, https://doi.org/10. 1109/TMECH.2013.2279751 [Accessed on 04 February 2020].
- [55] S. Gibb, H.M. La, T. Le, L. Nguyen, R. Schmid, N. Pham, Non-destructive evaluation sensor fusion with autonomous robotic system for civil infrastructure inspection, Journal of Field Robotics 35 (6) (2018) 988–1004, https://doi.org/10.1002/rob.21791 [Accessed on 01 March 2020].
- [56] T.H. Dinh, Q.P. Ha, H.M. La, computer vision-based method for concrete crack detection, in: proceedings of international conference on control, automation, robotics and vision (ICARCV), Phuket, Thailand 13-15 (Nov. 2016) 1–6, https:// doi.org/10.1109/ICARCV.2016.7838682 [Accessed on 15 February 2020].
- [57] U.H. Billah, H.M. La, A. Tavakkoli, N. Gucunski, Classification of concrete crack using deep residual networks, In: Proceedings of International Conference on Structural Health Monitoring (SHMII-9), St. Louis, MI, USA, 4–7 Aug. 2019. pp. 1–6. [Online], Retrieved from: [Accessed on 07 February 2020]. https://ara.cse. unr.edu/wp-content/uploads/2014/12/SHMII-9-Full-paper-Templatefinaly4.pdf.
- [58] S. Gibb, H.M. La, S. Louis, A genetic algorithm for convolutional network structure optimization for concrete crack detection, in: proceedings of IEEE congress on evolutionary computation (CEC), Rio de Janiero, Brazil, 8-13 (July 2018), pp. 1–8, https://doi.org/10.1109/CEC.2018.8477790 [Accessed on 05 February 2020].
- [59] U.H. Billah, A. Tavakkoli, H.M. La, Concrete crack pixel classification using an encoder-decoder based deep learning architecture, in: proceedings of international symposium on visual computing (ISVC), Lake Tahoe, NV, USA, 7-9 (Oct. 2019), pp. 593–604, https://doi.org/10.1007/978-3-030-33720-9 [Accessed on 06 February 2020].
- [60] Y.-J. Cha, W. Choi, O. Buyukozturk, Deep learning-based crack damage detection using convolutional neural networks, Computer-Aided Civil and Infrastructure Engineering 32 (5) (2017) 361–378, https://doi.org/10.1111/mice.12263 [Accessed on 07 May 2020].
- [61] G.H. Beckman, D. Polyzois, Y.-J. Cha, Deep learning-based automatic volumetric damage quantification using depth camera, Autom. Constr. 99 (2019) 114–124, https://doi.org/10.1016/j.autcon.2018.12.006 [Accessed on 07 May 2020].
- [62] Y.-J. Cha, W. Choi, G. Suh, S. Mahmoudkhani, O. Buyukozturk, Autonomous structural visual inspection using region-based deep learning for detecting multiple damage types, Computer Aided Civil Infrastructural Engineering 33 (2018) 731–747, https://doi.org/10.1111/mice.12334 [Accessed on 07 May 2020].
- [63] J. K. Alvarez and S. Kodagoda, Application of deep learning image-to-image transformation networks to GPR radargrams for sub-surface imaging in infrastructure monitoring, In: Proceedings of 13th International IEEE Conference on Industrial Electronics and Applications (ICIEA), Wuhan, China. 31 May - 2 June 2018. pp. 1-6. DOI: https://doi.org/10.1109/ICIEA.2018.8397788. [Accessed on 01 February 2020].
- [64] S. Khudoyarov, N. Kim, J.-J. Lee, Three-dimensional convolutional neural network-based underground object classification using three-dimensional ground penetrating radar, Structural Health Monitoring (2020) 1–10, https://doi.org/10. 1177/1475921720902700 [Accessed on 02 March 2020].
- [65] Z.W. Wang, M. Zhou, G.G. Slabaugh, J. Zhai, T. Fang, Automatic detection of bridge deck condition from ground penetrating radar images, IEEE Trans. Autom. Sci. Eng. 8 (3) (2011) 633–640, https://doi.org/10.1109/TASE.2010.2092428 [Accessed on 02 February 2020].
- [66] P. Gamba, S. Lossani, Neural detection of pipe signatures in ground penetrating radar images, IEEE Transactions on Geosciences and Remote Sensing 38 (2) (2000) 790–797, https://doi.org/10.1109/36.842008 [Accessed on 07 February 2020].
- [67] W. Al-Nuaimy, Y. Huang, M. Nakhkash, M.T.C. Fang, V.T. Nguyen, A. Eriksen, Automatic detection of buried utilities and solid objects with GPR using neural networks and pattern recognition, J. Appl. Geophys. 43 (2) (2000) 157–165, https://doi.org/10.1016/s0926-9851(99)00055-5 [Accessed on 06 February 2020].
- [68] S. Gibb and H. M. La, Automated rebar detection for ground penetrating radar, in: Proceedings of the 12th international symposium on visual computing, Las Vegas, NV, USA. Dec 12-14 2016. pp. 815–825.
- [69] H. Ahmed, H. M. La and N. Gucunski, Rebar Detection using Ground Penetrating Radar with State-of-the-Art Convolutional Neural Networks, In: Proceedings of the 9th International Conference on Structural Health Monitoring of Intelligent infrastructure (SHMII-9), St. Louis, MI, USA. 4–7 Aug. 2019. pp. 1–6. [Online]. Retrieved from: https://ara.cse.unr.edu/wp-content/uploads/2014/12/SHMII-GPR-Paper-Final-Version-4.pdf [Accessed on 07 February 2020].
- [70] H. Ahmed, H.M. La, G. Pekcan, rebar detection and localization for non-destructive infrastructure evaluation using deep residual networks, in: proceedings of the 14th international symposium on visual computing, Lake Tahoe, NV, USA. 7-9 (Oct. 2019) 1–6, https://doi.org/10.1007/978-3-030-33720-9\_49 [Accessed on 04 February 2020].
- [71] K. Dinh, N. Gucunski, T.H. Doung, An algorithm for automatic localization and detection of rebars from GPR data of concrete bridge decks, Autom. Constr. 89 (2018) 292–298, https://doi.org/10.1016/j.autcon.2018.02.017 [Accessed on 07 February 2020].
- [72] J. Yu, H. Chen, Q. Dou, J. Qin, P.-A. Heng, Automated melanoma recognition in Dermoscopy images via very deep residual networks, IEEE Trans. Med. Imaging 36 (4) (2017) 994–1015, https://doi.org/10.1109/TMI.2016.2642839 [Accessed on 10 February 2020].

- [73] Z. Zhang, Q. Liu, Y. Wang, Road extraction by deep residual U-net, IEEE Geosciences and Remote Sensing Letters 15 (5) (2018) 749-754, https://doi.org/ 10.1109/LGRS.2018.2802944 [Accessed on 12 February 2020].
- [74] J.-H. Kim and J.-S. Lee, Deep residual network with enhanced Upscaling module for super-resolution, in: Proceedings of IEEE international conference on computer vision workshop (ICCVW), Salt Lake City, UT, USA. 18-22 June 2018. pp. 913-922. Doi:https://doi.org/10.1109/CVPRW.2018.00124. [Accessed on 15
- [75] K. He, X. Zhang, S. Ren and J. Sun, Deep residual learning for image recognition, in: Proceedings of IEEE international conference on computer vision (ICCV), Las Vegas, NV, USA. 27-30 June 2016. pp. 770-778. DOI: https://doi.org/10.1109/ CVPR.2016.90. [Accessed on 20 February 2020].
- [76] G. Haung, Z. Liu, L. van der Maaten, K.Q. Weinberger, Densely Connected Convolutional Networks arXiv, p. 1608.06993, pp. 1-9, (2016) [Accessed on 16 February 20201.
- [77] K. He, X. Zhang, S. Ren and J. Sun, Deep Residual Learning for Image Recognition, arXiv: 1512.03385, pp. 1-12, 2015. [Accessed on 10 February 2020].
- [78] M. Boroumand, M. Chen, J. Fridich, Deep residual network for Steganalysis of digital images, IEEE Transactions on Information Forensics and Security 14 (5) (2019) 1181-1193, https://doi.org/10.1109/TIFS.2018.2871749 [Accessed on 13 February 2020].
- [79] C. Feichtenhofer, A. Pinz and R. P. Wildes, Spatiotemporal Residual Networks for Video Action Recognition, In: Proceedings of Neural Information Processing Systems, Barcelona, Spain. 5-10 Dec. pp. 1-9, 2016. ISBN: 978-1-5108-3881-9. [Accessed on 14 February 2020].
- [80] M. Zhai, X. Xiang, R. Zhang, N. Lv, A. Saddik, Learning optical flow using deep dilated residual networks, IEEE Access 7 (2019) 22566-22578, https://doi.org/ 10.1109/ACCESS.2019.2898988 [Accessed on 16 February 2020].
- [81] J. Li, G. Li, H. Fan, Image Dehazing using residual based deep CNN, IEEE Access 6 (2018) 26831-26844, https://doi.org/10.1109/ACCESS.2018.2833888 [Accessed on 15 February 2020].
- [82] M. Paoletti, J.M. Haut, R. Fernandez-Beltran, A.J. Plaza, Deep pyramidal residual networks for spectral spatial Hyperspectral image classification, IEEE Trans. Geosci. Remote Sens. 57 (2) (2019) 740-754, https://doi.org/10.1109/TGRS. 2018.2860125 [Accessed on 12 February 2020].
- [83] M. Zhao, M. Kang, B. Tang, M. Pecht, Multiple wavelet coefficients fusion in deep residual networks for fault diagnosis, IEEE Transactions on Fault Diagnosis 66 (6) (2019) 4096-4707, https://doi.org/10.1109/TIE.2018.2866050 [Accessed on 17 February 2020].
- [84] H. Li, F. Fang, K. Mei and G. Zhang, Multi-scale residual network for image superresolution, in: Proceedings of European conference on computer vision (ECCV), Munich, Germany. 8-14 Sept. 2018. pp. 1-16. DOI: https://doi.org/10.1007/978-3-030-01246-5. [Accessed on 17 February 2020].
- [85] K. Zhang, M. Sun, T.S. Han, X. Yuan, L. Guo, T. Liu, Residual networks of residual networks: multilevel residual networks. IEEE Transactions on Circuits and Systems for Video Technology 28 (6) (2018) 133–1314, https://doi.org/10.1109/TCSVT. 2017.2654543 [Accessed on 16 February 2020].
- [86] R. Ali, Y.-C. Cha, Subsurface damage detection of a steel bridge using deep learning and uncooled micro-bolometer, Constr. Build. Mater. 226 (2019) 276-287, https://doi.org/10.1016/j.conbuildmat.2019.07.293 [Accessed on 12] February 2020].
- [87] J.K. Hart, K.C. Rose, A. Clayton, K. Martinez, Englacial and subglacial water flow at Skalafellsjokull, Iceland derived from ground penetrating radar, in situ Glacsweb probe and borehole water level measurements, Earth Surf. Process. Landf. 40 (2015) 2071-2083, https://doi.org/10.1002/esp.3783 [Accessed on 20 February 2020].
- [88] M. Leopold, M.W. Williams, J. Volkel, D. Dethier, Internal structure of the green Lake 5 rock glacier, Colorado front range, USA, Permafr. Periglac. Process. 22 (2) (2011) 107-119, https://doi.org/10.1002/ppp.706 [Accessed on 21 February 20201
- [89] M. Christie, G.P. Tsoflias, D.F. Stockli, A.B. Ross, Assessing fault displacement and off-fault deformation in an extensional tectonic setting using 3-D ground-penetrating radar imaging, J. Appl. Geophys. 68 (1) (2009) 9-16, https://doi.org/10. 1016/j.jappgeo.2008.10.013 [Accessed on 22 February 2020].
- [90] J.N. Malik, A.K. Sahoo, A.A. Shah, D.P. Shinde, N. Juyal, A.K. Singhvi, Paleoseismic evidence from trench investigation along Hajipur fault, Himalayan frontal thrust, NW Himalaya: implications of the faulting pattern on landscape evolution and seismic hazard, J. Struct. Geol. 32 (2010) 350-361, https://doi.org/ 10.1016/j.jsg.2010.01.005 [Accessed on 20 February 2020].
- [91] J. Plado, I. Sibul, M. Mustasaar, Ground-penetrating radar study of the Rahivere peat bog, eastern Estonia, Estonian Journal of Earth Sciences 60 (1) (2011) 31-42, ttps://doi.org/10.3176/earth.2011.1.03 [Accessed on 21 February 2020].
- [92] M.A.T. de Oliviera, J.L. Porsani, G.L. de Lima, V. Jeske-Peiruscha, H. Behling,

- Upper Pliestocene to Holocene peatland evolution in southern Brazilian highlands as depicted by radar stratigraphy, sedimentology and palynology, Quarternary Research 77 (3) (2012) 397-407, https://doi.org/10.1016/j.yqres.2011.12.006 [Accessed on 22 February 2020].
- T. Tamura, F. Murakami, F. Nanayama, K. Watanabe, Y. Saito, Ground penetrating radar profiles of Holocene raised-beach deposits in the Kujukuri strand plain, Pacific coast of eastern Japan, Mar. Geol. 248 (1-2) (2008) 11-27, http org/10.1016/j.margeo.2007.10.002 [Accessed on 22 February 2020].
- [94] L.B. Clemmenson, L. Nielsen, M. Bendixen, A. Murray, Morphology and sedimentary architecture of a beach-ridge system Anholt, the Kattegat Sea: a record of punctuated coastal progradation and sea-level change over the past - 1000 years, Boreas 41 (2012) 422–434, https://doi.org/10.1111/j.1502-3885.2012.00250.x [Accessed on 20 February 2020].
- [95] P.L. Gibbard, R.G. West, S. Boreham, C.J. Rolfe, Late middle Pleistocene icemarginal sedimentation in East Anglia, England, Boreas 41 (3) (2011) 319-336, https://doi.org/10.1111/j.1502-3885.2011.00236.x [Accessed on 22 February
- [96] S.H. Ward, R.J. Phillips, G.F. Adams, W.E. Brown, R.E. Eggleton, P. Jackson, R. Jordan, W.I. Linlor, W.J. Peeples, L.J. Porcello, J. Ryu, G. Schaber, W.R. Sill, S.H. Thompson, J.S. Zelenka, Apollo lunar sounder experiment, in Apollo 17: Preliminary Science Report, Washington, DC: NASA, 1973. Report no. NASA SP-330. [Online], Retrieved from: https://www.hq.nasa.gov/alsj/a17/as17psr.pdf.
- [97] R.M. Morey, Continuous subsurface profiling by impulse radar, Proceedings of Engineering Foundations Conference on Subsurface Exploration for Underground Excavations and Heavy Constructions, 1974, pp. 213-232, , https:/ 1080/00288306.1985.10422540 [Accessed on 21 February 2020].
- [98] J.L. Davis, A.P. Annan, Ground penetrating radar for high resolution mapping of soil and rock stratigraphy, Geophyiscal Prospecting 37 (1989) 531-551, https 478.1989.tb02221.x [Accessed on 24 February 2020].
- [99] H. K. Chlaib, H. Mahdi, H. Al-Shukri, M. M. Su, A. Catakli and N. Abd, Using ground penetrating radar in levee assessment to detect small scale animal burrows, J. Appl. Geophys., vol. 103, pp. 121–131, 2014. DOI: https://doi.org/10.1016/j. ppgeo.2014.01.011. [Accessed on 22 February 2020].
- L.B. Conyers, D. Goodman, Ground Penetrating Radar- an Introduction for Archaeologists, Altamira Press, London, UK, 1997 [ISBN: 0-761-8928-5. Accessed on 22 February 2020].
- [101] A.P. Annan, Chapter 11: Ground penetrating radar, in: D.K. Butler (Ed.), Near Surface Geophysics, Elsevier, Amsterdam, 2005, pp. 3–40, , https 190/1.9781560801719.ch11 [Accessed on 20 February 2020].
- [102] A.P. Annan, Electromagnetic Principles of Ground Penetrating Radar, in Ground Penetrating Radar: Theory and Applications, Elsevier, Amsterdam, 2009, pp. 3–40, https://doi.org/10.1016/B978-0-444-53348-7.00001-6 [Accessed on 20 February
- [103] A. Neal, Ground penetrating radar and its use in sedimentology: principles, problems and progress, Earth-Sci. Rev., vol. 66, pp. 261–330, 2004. DOI: https://doi. org/10.1016/j.earscirev.2004.01.004. [Accessed on 21 February 2020].
- M. Robinson, C. Bristow, J. McKinley, A. Ruffell, Ground Penetrating Radar, Geomorphological Techniques, vol. 1, no. 5.5, pp. 1-26, (2013) ISSN: 2047-0371. Accessed on 22 February 2020]..
- [105] H. M. Jol, C. S. Bristow, D. G. Smith, B. Junck and P. Putnam, Stratigraphic imaging of the Navajo sandstone using ground-penetrating radar, Lead. Edge, pp. 882-887, 2003. DOI: https://doi.org/10.1190/1.1614162. [Accessed on 23 February 20201.
- [106] Geophysical Inc, Explore Our Range of Products, Retrieved from https://www. geophysical.com/products, (2020) [Accessed on 2 May 2020].
  [107] Sensors & Software Inc, What is GPR? Retrieved from https://www.sensoft.ca/
- log/what-is-gpr/ 2020. [Accessed on 2 May 2020].
- US Radar Inc, Products, Retrieved from https://usradar.com/ground-penetratingadar-products/ 2020. [Accessed on 2 May 2020].
- [109] I.G. Systems, Online, Retrieved from: https://www.idscorporation.com/.
   [110] L. Derczynski, Complementarity, F-score, and NLP Evaluation, Proceedings of the 10th International Conference on Language Resources and Evaluation, Portoroz, Slovenia. 23–28 May 2016. pp. 261–266, 2016 ISBN: 978-2-9517408-9-1. [Accessed on 25 February 2020].
- [111] Q. Dou, L. Wei, D. R. Magee and A. G. Cohn, Real-time hyperbola recognition and fitting in GPR data, IEEE Transactions on Geosciences and Remote Sensing, vol. 55, no. 1, pp. 51-63, 2017. DOI: https://doi.org/10.1109/TGRS.2016.2592679. [Accessed on 24 February 2020].
- [112] H. Harkat, A. E. Ruano, M. G. Ruano and S. D. Bennani, GPR target detection using a neural network classifier designed by a multi-objective genetic algorithm, Applied Soft Computing Journal, vol. 79, pp. 310-325, 2019. DOI: https://doi. org/10.1016/j.asoc.2019.03.030. [Accessed on 22 February 2020].